MARIA S. MERIAN-Berichte

Evolution of the Heligoland Glaciotectonic complex, North Sea, and total lateral extent and age of the giant buried Tampen Slide off Norway

Cruise No. MSM 98/2

26.01.2021 – 22.02.2021
Emden – Emden (Germany)
(GPF20-3_073)

AUTHORS

Dr. Jens Schneider v. Deimling
Institut für Geowissenschaften, CAU Kiel

and scientific party

2022

Inhalt

1 Cruise Summary

1.1 Summary in English

During MSM98/2 two independent objectives were pursued. In the first cruise section, the Tampen submarine landslide on the Norwegian continental slope was seismically mapped to determine its extent and volume. Initially, the slide could be clearly traced from the headwall downslope in our multichannel seismic data. However, the corresponding sequence partially struck out on its way to Aegir Ridge. Further seismic surveys in and along Aegir Ridge revealed several turbidite layers. At the shoulder of the ridge, the hydroacoustic imaging identified layers within the first meters in a striking facies and gravity cores were successfully taken here. In total, three turbidite layers could be clearly delineated in the several meter long cores. Their dating will provide information about the age of the respective turbidites, which will be fundamental for reconstruction of landslide history.

In the second cruise section, the Heligoland Glaciotectonic Complex (HGC) was targeted using seismic and hydroacoustic methods to reconstruct the advances and retreats of ice sheets in the southeastern North Sea during the Quaternary. Aiming for a combined profile line spacing of only 400 m, we were able to generate a very high-density subbottom data set. Thrust sheets and faults are imaged well in our data, although further processing is needed to reduce shallow water artefacts. From the new data, we know that the HGC extends farther than previously thought and we established a seamless connection to the previous high-resolution data set in the region. Some thrust sheets were cut and eroded by subglacial meltwater channels (so-called tunnel valleys) providing the relative temporal sequence. Sporadically, we were able to identify small near-surface channels that lie only 1-2 m below the seafloor and are cut only few meters into the ground. This data set provides the basis to further analyse the formation of the HGC and its interaction with the large tunnel valley in the region. We will be able to update the spatial distribution of tunnel valleys in the area. Additionally, we sailed dedicated profiles along the course of these tunnel valleys. Such data has been non-existent for tunnel valleys and holds the potential to shed light on their formation and infill mechanisms. Furthermore, we examined the seafloor surface and shallow subsurface for possible degassing structures, but no evidence of fluid seepage and pockmark genesis was found.

1.2 Zusammenfassung

Während MSM98/2 wurden zwei unabhängige Ziele verfolgt. Im ersten Fahrtschnitt wurde die Tampen-Rutschung am norwegischen Kontinentalhang seismisch kartiert um ihre Ausdehnung und ihr Volumen bestimmen zu können. Zunächst konnte die Rutschung von der Abrisskante in unseren Mehrkanalseismikdaten klar verfolgt werden. Jedoch strich die entsprechende Sequenz auf dem Weg zum Aegir Ridge partiell aus. Weitere seismische Untersuchungen im und am Aegir Ridge zeigten verschiedene Turbiditlagen. An der Schulter des Rückens konnten im hydroakustischen Abbild mehrere Lagen auf den ersten Metern in einer ausstreichenden Fazies identifiziert werden und es gelang hier mehrere Schwerelote abzuteufen. Insgesamt konnten in den mehrere Meter langen Kernen drei Turbiditlagen klar voneinander abgegrenzt werden. Deren Datierung wird Aufschluss über das Alter der jeweiligen Turbidite geben.

Im zweiten Fahrtabschnitt wurde der Helgoländer glaziotektonische Komplex (HGC) mit seismischen und hydroakustischen Methoden abgebildet, um das Vorrücken und Zurückweichen von Eismassen während des Quartärs zu rekonstruieren. Mit einem Profillinienabstand von nur 400 m gelang es uns einen hochauflösenden Datensatz mit sehr hoher Profildichte zu generieren. Die Schuppungen und Verwerfungen zeichnen sich in unseren Daten gut ab und reichen weiter, als bisher angenommen. Dennoch wird ein speziell auf Flachwasser abgestimmtes Prozessing nötig sein, um Artefakte zu unterdrücken und die Interpretation zu vereinfachen. Einige der Schuppungen wurden von subglazialen Schmelzwasserrinnen (sog. Tunneltälern) geschnitten und erodiert – eine relative zeitliche Abfolge wird so schnell klar. Stellenweise konnten wir oberflächennahe Kanäle identifizieren, welche nur 1-2 m unter dem Meeresboden liegen und wenige Meter in den Boden eingeschnitten sind. Generell erlauben die Daten eine weitere Analyse der Entstehung des glaziotektonischen Komplexes und seine Interaktion mit den großen Tunneltälern der Region. Auf dieser Basis werden wir die Verteilung von Tunneltälern in der Region neu bewerten und aktualisieren können. Zusätzlich sind wir auf Basis bestehender Daten Profile entlang dieser Tunneltäler gefahren. Solch hoch aufgelöste Daten der Tunneltäler wurden bisher noch nicht erhoben und sie haben das Potential neue Erkenntnisse über die Entstehung und Füllung der Tunneltäler zu liefern. Des Weiteren untersuchten wir die Meeresbodenoberfläche und den flachen Untergrund in Hinblick auf mögliche Entgasungsstrukturen, jedoch konnten keine Hinweise auf Fluidaustritt und die Entstehung von Pockmarks gefunden werden.

2 Participants

2.1 Principal Investigators

Name	Institution
Krastel, Sebastian, Prof.	CAU
Talling, Peter, Prof.	Durham University
Haflidason, Haflidi, Prof.	Bergen University

2.2 Scientific Party

Name	Discipline	Institution
Schneider von Deimling, Jens, Dr.	Chief Scientist	CAU
Lohrberg, Arne	Seismics/Hydroacoustic	CAU
Tang, Qinqin	Seismics/Hydroacoustics	CAU
Grob, Henrik	Seismics/Hydroacoustics	CAU
Hildebrandt, Stine	Seismics/Hydroacoustics	ZBSA
Jähmlich, Heiko	Technician	CAU
Heinrich, Sven	Technician	CAU
Wallmeier, Carolin	Seismics/Hydroacoustics	CAU
Hinz, Anina	Seismics/Hydroacoustics	GEOMAR
Gross, Katharina	Sedimentology	CAU
Schmitz, Alexander	Sedimentology	CAU
Scheffler, Janne	Sedimentology	CAU

2.3 Participating Institutions

GEOMAR	Helmholtz-Zentrum für Ozeanforschung Kiel
CAU	Christian-Albrechts-Universität zu Kiel
ZBSA	Center for Baltic and Scandinavian Archaeology

3 Research Program

3.1 Description of the Work Areas

German Bight

Studies investigating the shelf architecture northeast of Heligoland have shown major subglacial tunnel valleys and a proglacial glaciotectonic complex in the area northeast of Heligoland dating back to the Elsterian glaciation or earlier (Winsemann et al., 2020; Lohrberg et al., 2020). Their results show that large-scale subglacial drainage systems resulted in deep and wide valleys. Following the Elsterian glaciation, these large glaciogenic landforms have been filled and overridden during the Saalian glaciation, such that only erosional surfaces remain at their top. Late Pleistocene sand and gravel deposits drape these erosional surfaces and build the basis for drainage patterns during and at the end of the last glacial maximum into the North Sea. The resulting channels are thus part of a highly dynamic landscape that formed during the late Pleistocene.

The Tampen Slide and Aegir Ridge

A series of very large volume submarine slides have been recognised along the Norwegian Margin (e.g. King et al. 1996; Laberg and Vorren 2000; Nygård et al. 2005; Pope et al. 2018). The most recent of these giant landslides, the 8.2 ka Storegga Slide, resulted in a catastrophic tsunami whose impact was felt as far south as Denmark. The Tampen Slide, the mega-slide that preceded the Storegga Slide, is buried beneath up to 450 m of sediment near its headwall. The headwall area of the Tampen Slide has been extensively studied using 2D and 3D seismic surveys, most recently by Barrett et al. (2020), however the full lateral extent and volume of the Tampen Slide remain poorly constrained. Moreover, the burial of the Tampen Slide, together with the partial subsequent remobilization of its deposits by the Storegga Slide, have complicated its dating, with past work relying mainly on the ages assigned to regional seismic reflectors (Nygård et al. 2005) and a single piston core recovered by the Marion Dufresne (MD99-2283, Lekens et al. 2009).

The Aegir Ridge, an extinct spreading ridge in the Norway Basin, is located ~300 km northwest of the Tampen Slide headwall. Multiple stacked turbidite bodies, including some of giant volume possibly exceeding that of the Storegga Slide, have been documented within the Aegir Ridge (Hjelstuen and Andreasson, 2015; Watts 2019). Their age and stratigraphic relationship to the Tampen Slide, however, remains unclear.

3.2 Aims of the Cruise

The cruise MSM98/2 had two independent objectives. By means of seismic measurements and sampling by gravity cores, the extent, volume and age of the Tampen landslide on the Norwegian continental slope will be determined. This is crucial for the assessment of tsunami hazards. So far, it has been postulated that landslides off Norway occur shortly after the transition to an interglacial. The Tampen landslide is the last known major landslide before the 8.2 ka old Storegga landslide; its age has previously been estimated at 130 ka. We will investigate whether a 55-60 ka old mega-turbidite on Aegir Ridge is related to the Tampen slide or another large slide of unknown origin. Both possibilities suggest that models for linking mega-slides to glacial and climatic cycles are incomplete. However, there are no seismic profiles to date to correlate the Aegir mega-turbidite with the headwall of the Tampen landslide.

A study north of Heligoland aims to image a glaciotectonic complex to reconstruct ice advances and retreats during the Quaternary. The glaciotectonic complex is known (Winsemann et al., 2020); however, the available data do not allow a detailed description of its architecture, including the lateral extent of the different décollements and the thrust directions in different areas. To reconstruct the complex and the margins of the ice sheet during glacial cycles, we plan to record dense seismic profiles. The resulting data will additionally allow for further characterization of the tunnel valleys interacting with the glaciotectonic complex.

3.3 Agenda of the Cruise

The cruise was conducted by a limited number of 13 scientists from 3 institutes on board of the MSM (Christian-Albrechts-Universität zu Kiel, GEOMAR Helmholtz Centre for Ocean Research Kiel, Center for Baltic and Scandinavian Archaeology). After a 4-day quarantine and COVID-19 tests in a hotel in Leer we boarded the ship on 24th of January and the cruise ended on 22nd February in Emden. Except for minor technical issues the cruise was be conducted as planned during fairly pleasant weather conditions when considering the season and working areas. First, we sailed to the northerly working area near the polar circle (Fig. 3.1). The second half of the cruise was conducted in the German Bight subsequently.

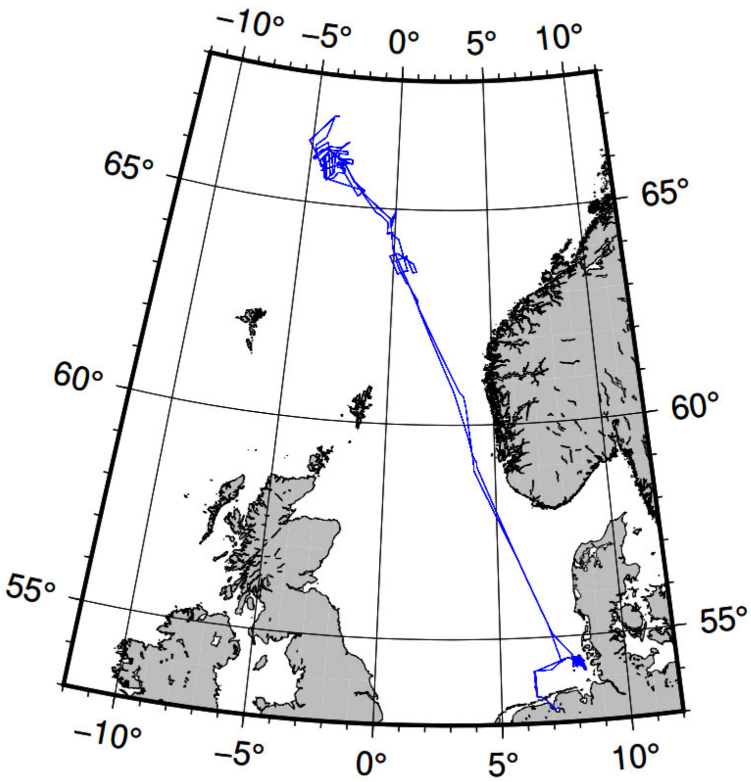

Fig. 3.1 Track chart of MSM98/2 ships track (blue) connecting the two working areas. One is located offshore Norway extending to Aegir ridge, the other in the German Bight between the islands of Sylt and Heligoland (Projection UTM32N).

4 Narrative of the Cruise

We departed port of EMDEN on Tuesday, 26.01.2021, as scheduled at 07:30 UTC and ran first tests of our hydroacoustic equipment near Heligoland. Then we steamed north and entered Norwegian waters on Wednesday 27.01 at 05:40 UTC. After 2.5 days we arrived in the first working area near the Tampen landslide headwall area on Thursday 28.01 around 13:00 UTC. Here we deployed the seismic streamer and our seismic source. After some technical problems, we began with a softstart in the late afternoon and subsequently started our seismic surveying profile with the aim to connect the Tampen headwall area with Aegir ridge. In the evening of Friday, 29.01, the weather unexpectedly deteriorated fast with waves up to 6 m high and wind gusts of 26 m/s; the streamer and airgun had to be recovered. We ran dedicated subbottom profiler and multibeam echosounder profiles on Saturday 30.01 and Sunday 31.01 to identify suitable gravity corer locations within the Aegir ridge trough and adjacent areas. During the very limited amount of daylight we gathered 4 gravity cores on Monday 01.02 and Tuesday 02.02 which recovered up to 5.5 m of fine grained material. During night, we extended our subbottom profiles. With decreasing swells we proceeded with the multichannel airgun seismics to correlate the landward side of the landslide deposits heading towards the Aegir ridge. We faced major technical problems on the morning of Wednesday 03.02 and stopped the survey at 10:22 UTC. The repair took several hours during which the Danish royal airforce visited us by helicopter and took some pictures of the vessel. Around 14:00 UTC we re-deployed the repaired streamer but two hours later the wind increased again to 20 m/s. Therefore, we recovered streamer and airgun and adjusted our survey plan. The following days, we acquired seismic profiles aligned with the direction of wind and waves at day time and reserved time to search for gravity corer positions during the nights while sailing in the opposite direction. This strategy was successful and we found some excellent shallow sediment pinch-out areas suitable for gravity coring. Three gravity cores with up to 7.3 m in length were recovered from a basin on a morphological high northwest of the ridge axis on Friday 05.02. We found at least two turbidites in one of the cores. On Friday night we continued the seismic surveying, had to re-deployed and soft started on Saturday 06.02 17:00 UTC in between, and finished our program at Aegir ridge Sunday 07.02 8:00 UTC. At night, we steamed upslope and deployed our streamer again to refine the previously found Tampen slide pinch-out area likely caused by an overall morphological high at depth of unknown origin. We continued seismic profiling here until Wednesday 10.02 05:00 UTC under fairly calm weather conditions for the first time during this cruise. We sailed a roll calibration for the deep water multibeam echosounder in 1500 m water depth, and began the transit back towards the continental shelve to head to our second research area in the German Bight. After steaming for two days, during which the seismic equipment was heavily tested on deck, we reached the second working area between the islands Sylt and Heligoland on Friday 12.02. We deployed the streamer and soft-started the airgun to begin seismic profiling at 9:55 UTC. This time, a Micro GI airgun was our source. It was operated at only 130 bar to adapt for the shallow water. The new PARASOUND system on board was fine-tuned for optimal imaging of the shallow palaeo landscape in parallel. Given the pleasant weather situation with a blocking high over Denmark and resulting easterly winds and minimum fetch for building waves, the seismic profiling lasted until Friday 19.02 09:30 UTC without technical problems. We only interrupted once for airgun maintenance reasons on Monday at 12:00 UTC as we had to replace O-rings as a precaution due to the high shot rate.

We installed our NORBIT multibeam echosounder in the ship's moonpool on the 19th noon time for the first time and ran habitat mapping surveys with NORBIT's multifrequency prototype system. We first had to calibrate the Applanix inertial navigation system on 19.02 13:30 UTC by sailing 'fast eights' for one hour. This task completed, we ran densely spaced survey lines to cover a part of the previous seismic working area until 20.02 noon time. Next, we took four van-Veen grab samples to ground-truth the habitat mapping survey. We left the working area in the evening and sailed to the 'wreck' calibration site 22 nm northwest of Heligoland, where we calibrated our multibeam, starting at 22:00 UTC. Subsequently, we conducted a multibeam echosounder survey around the wreck. On Sunday 21.02 14:00 UTC we finished the multifrequency multibeam echosounder surveying and recovered our device from the moonpool. Parasound and EM712 were continued until 21:00 UTC when we stopped the scientific program and started steaming back towards Emden. Finally, the scientific/technical party disembarked and left the vessel at 14:30 UTC on 22.02 to head back towards Kiel.

5 Preliminary Results

5.1 Multichannel seismics

(A. Lohrberg, H. Grob, K.-F. Lenz)

5.1.1 System overview and processing

During MSM98/2, we used the Geometric GeoEel 2D high-resolution multichannel seismic reflection system from CAU Kiel for seismic profiling. For our work off the Norwegian continental margin, we used a Sercel GI Gun with 2x 1.7 L in harmonic mode as our seismic source. In the very shallow waters of the German Bight we deployed a Sercel Micro GI gun with 2x 0.1L in harmonic mode.

In both surveys, the GI Gun was deployed at the portside pulser beam and towed 19.2 m behind the vessel. It was connected to a traverse bow, with the GI Gun hanging on two chains 70 cm beneath the bow. We mounted the system to a buoy attached to the airgun traverse bow with ~80 cm long ropes. Thus, the GI Gun was towed ~1.6 m below the water surface. The injector delay of the GI gun was set to 50 ms for the P1000-P2000 surveys and 48 ms for the P3000-P5000 surveys and 25 ms for the P6000-P7000 surveys. Air pressure was generated by the onboard Sauer&Sohn compressors and fed the GI Gun with 150 bar for the P1000-P5000 surveys and 130 bar for the P6000-P7000 surveys. The gun was shot every 6/6.5 seconds during P1000-P6000 and every 2.5 seconds during P6000-P7000. The GI Guns were frequently monitored and checked in detail before deployment. Between P6000 and P7000, all sealings of the Micro GI Gun were replaced due to hitting a maximum recommended shot number of 100,000 shots.

At the beginning of each deployment and after every interruption of surveys, we performed a soft start. During this soft start, the gun pressure was slowly increased over 20 minutes.

Geometrics GeoEel Solid high-resolution streamer system

To record the seismic signals, a Geometrics GeoEel digital solid-state streamer was used during all surveys. The system consists of a tow cable (39.2 m in water), two vibration insolation units (10 m long) at the head and the rear of the streamer, and 7 active sections (each 12.5 m). Between sections 3 and 4, a 1.562 m long bird control unit was installed. One active section of the streamer system contains 8 channels (channel spacing of 1.5625 m) resulting in 56 active channels within the streamer. One AD digitizer module at the beginning of each active section digitizes the analog data from the hydrophones. These AD digitizer modules are small Linux computers that transfer the data through the streamer via Ethernet. Communication between the AD digitizer modules and the recording system in the lab works via TCP/IP network. A repeater was located between the deck cable and the tow cable (Lead-In). The Streamer Power Supply Unit (SPSU) manages the power supply and communication between the recording system and the AD digitizer modules. Data were recorded with acquisition software provided by Geometrics. The analogue signals were digitized with 2 kHz. The data were recorded as multiplexed SEG-D. The recording length was set to 3 s for surveys P1000-P5000 and 1.5 s for P6000-P7000. One SEG-D file was generated per shot. The acquisition PC allowed on-profile monitoring by displaying shot gathers, a noise window, and the frequency spectrum of each shot. The cycle time of the shots was also displayed for control. The software also allows on-profile NMO-Correction and stacking of data for displaying stacked sections. Several log files list parameters such as shot time and shot position.

Bird Controller

Two Oyo Geospace Bird/Remote Units (RUs) were deployed with the streamer. The birds were attached to the vibration isolation unit at the lead in of the streamer system and to a 1.5625 m long bird section between the streamer sections 3 and 4. All RUs have adjustable wings and are controlled by a bird controller in the seismic lab. Controller and RUs communicate via communication coils nested within the anti-vibration units and the bird sections. A twisted pair wire within the deck cable connects the controller and coils. Designated streamer depth was set to 3.0 m. The RUs thus forced the streamer to the chosen depth by adjusting the wing angles accordingly. The birds were deployed at the beginning of seismic surveying but no scanning of the birds was carried out during the survey, as bird scans can cause major interference with the acquisition system. The birds worked very reliably and kept the streamer at its designated depth.

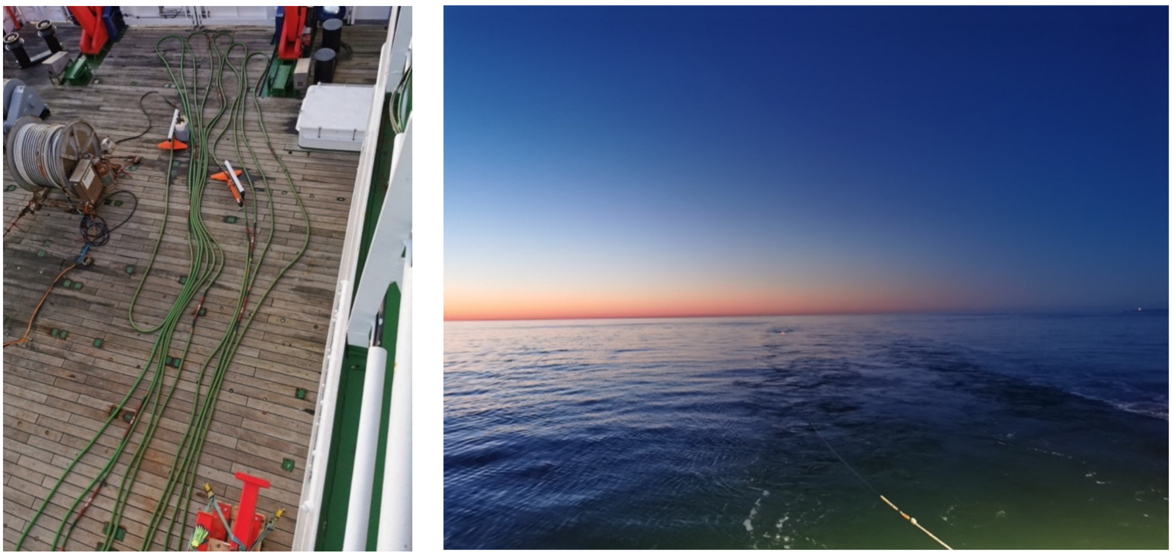

Fig. 5.1 Left: Streamer ready for deployment with two birds for depth control. Right: Streamer and gun in water during very calm sea in the morning close to Heligoland.

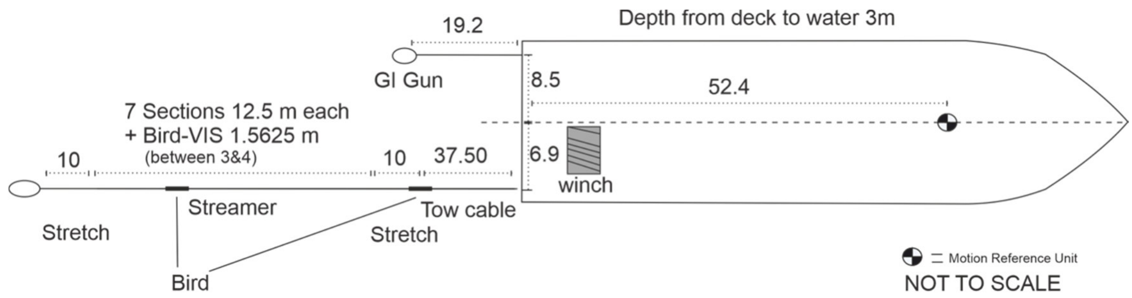

Fig. 5.2 Deck, Streamer and GI-Gun layout during Cruise MSM98/2.

Triggering

For triggering the systems, a University of Kiel custom built trigger and gun amplifier unit was used. Due to changing water depths, the shot rate varied for surveys P1000-P5000.

5.1.2 Results Tampen Slide – Aegir ridge

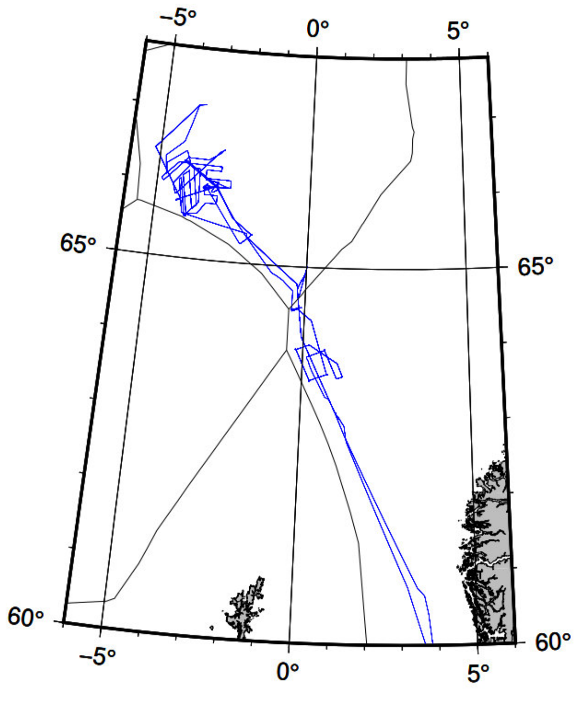

Fig. 5.3 Subplot track chart of MSM98/2 (blue) outlining the Tampen slide and Aegir ridge research area off Norway. (Projection UTM32N).

The first study area stretched from the continental margin west of Norway to the Aegir Ridge in the North Atlantic between Iceland and Norway (Fig. 5.3, 5.4). Two seismic lines are shown in Figures 5.5 and 5.6 at the continental slope and at the Aegir Ridge, respectively.

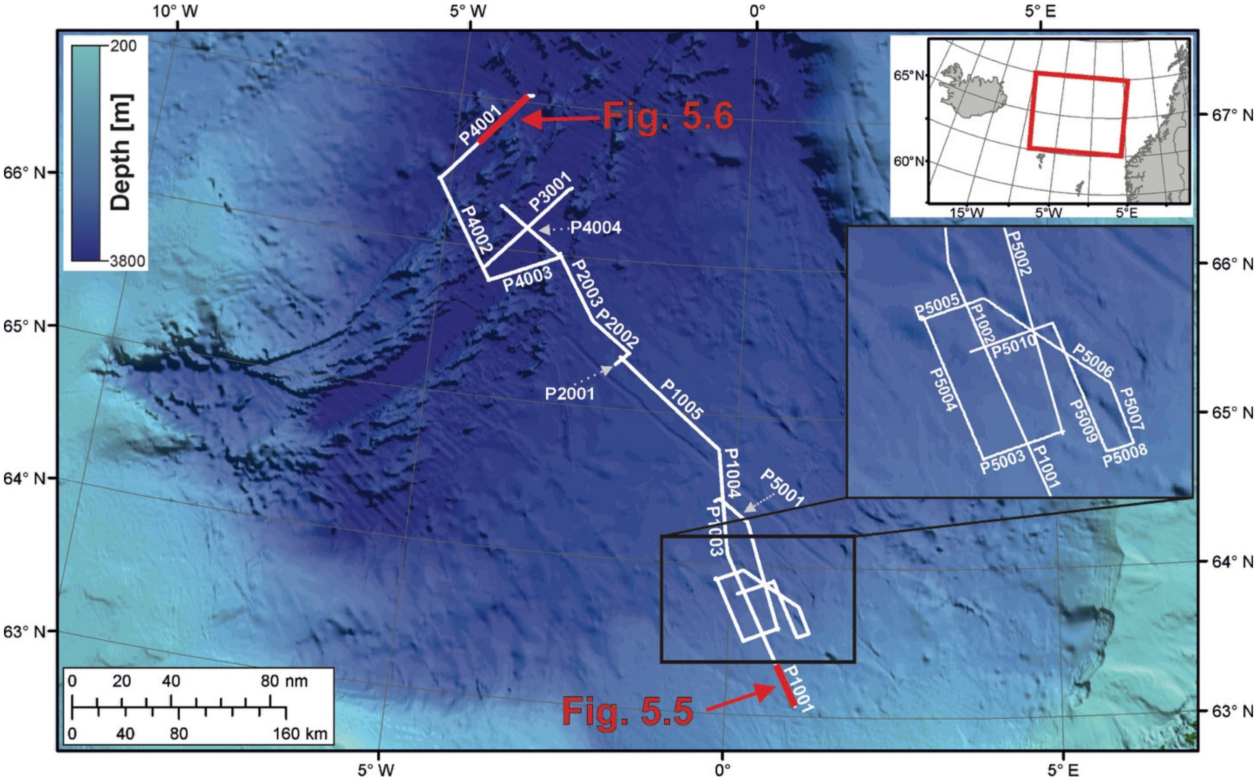

Fig. 5.4 Seismic lines acquired in the Tampen study area. The GEBCO bathymetry grid is used for background.

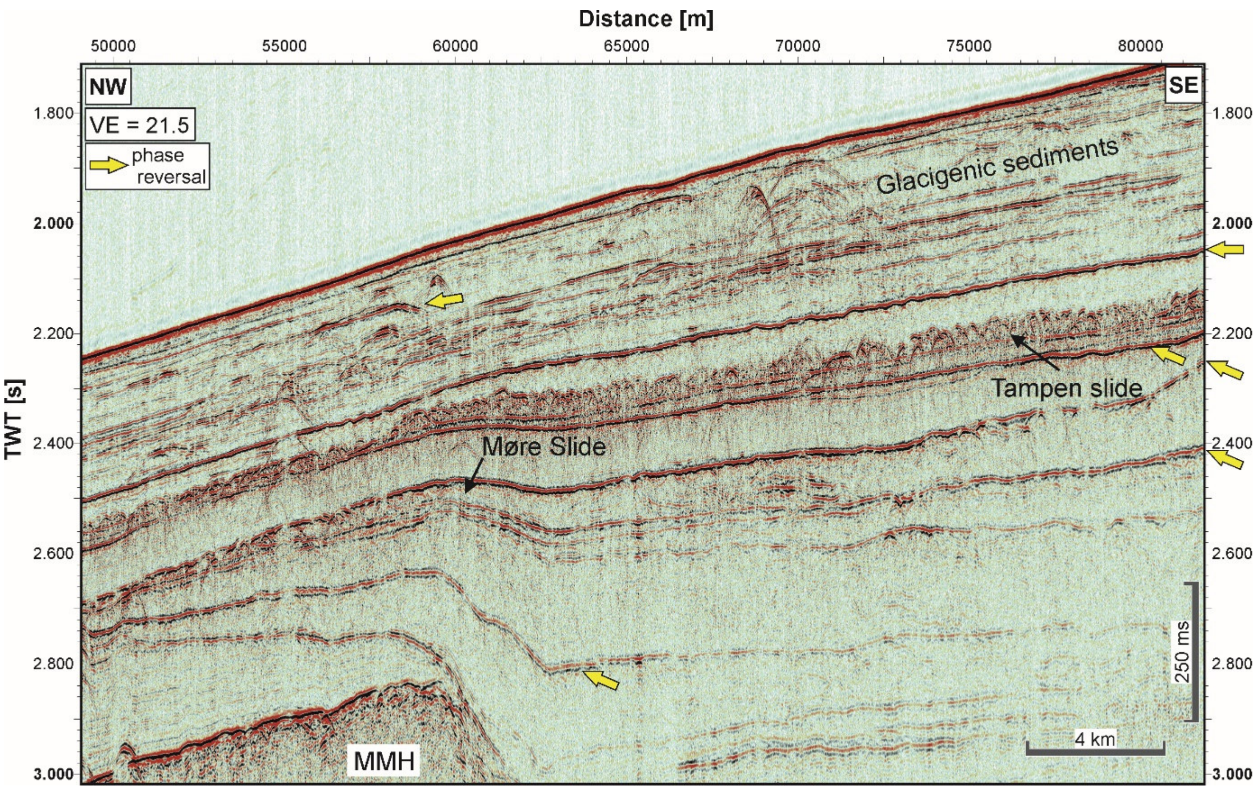

bathymetry.

Fig. 5.5 A part of profile P1001 at the continental slope west of Norway. The profile runs from southeast to northwest and crosses the Møre Marginal High (MMH). For location see Fig. 5.4.

A first part of profile 1001 is shown in Fig. 5.5 that runs along the continental slope. The line is characterised by the Møre Marginal High (MMH) at c. 2.9 s in the northwest and by a general stratification following the inclined seafloor. Prominent high-amplitude reflections confine stratigraphic low-amplitude units with minor stratification between 2-3 s TWT in the southeast. These prominent reflections are occasionally phase-reversed as indicated by yellow arrows (Fig. 5.5). Up to a prominent, phase-reversed reflection at c. 2.3 s and 60,000 m distance, reflections beneath are bent upwards as response to the morphologic elevation of the MMH. Above this reflection the bending diminishes, amplitudes increase slightly and the stratification becomes more pronounced. Major shallow diffractions and minor inclined reflections interrupt the overall impression of good stratification in the uppermost unit.

The most outstanding feature in Fig. 5.5 is a series of chaotic, high-amplitude reflections in conjunction with a high amount of diffractions. This feature is marked as Tampen Slide according to Barret et al. (2020). The Tampen Slide can be traced along downslope and thins slightly where the MMH builds up. The Tampen Slide is apparently emphasised by its seismic characteristic.

Besides the Tampen Slide we can also resolve the Møre Slide based on comparison with Barrett et al. (2020). At the build up of the MMH chaotic reflections dominate the seismic image at c. 60,000 m distance and 2.54 s TWT. Further downslope the Møre Slide thins clearly while upslope the seismic facies is characterised by decrease in amplitude. As described above, the uppermost unit is dominated in places by inclined reflections and diffractions. Barrett et al. (2020) describe these deposits as glaciogenic sediments.

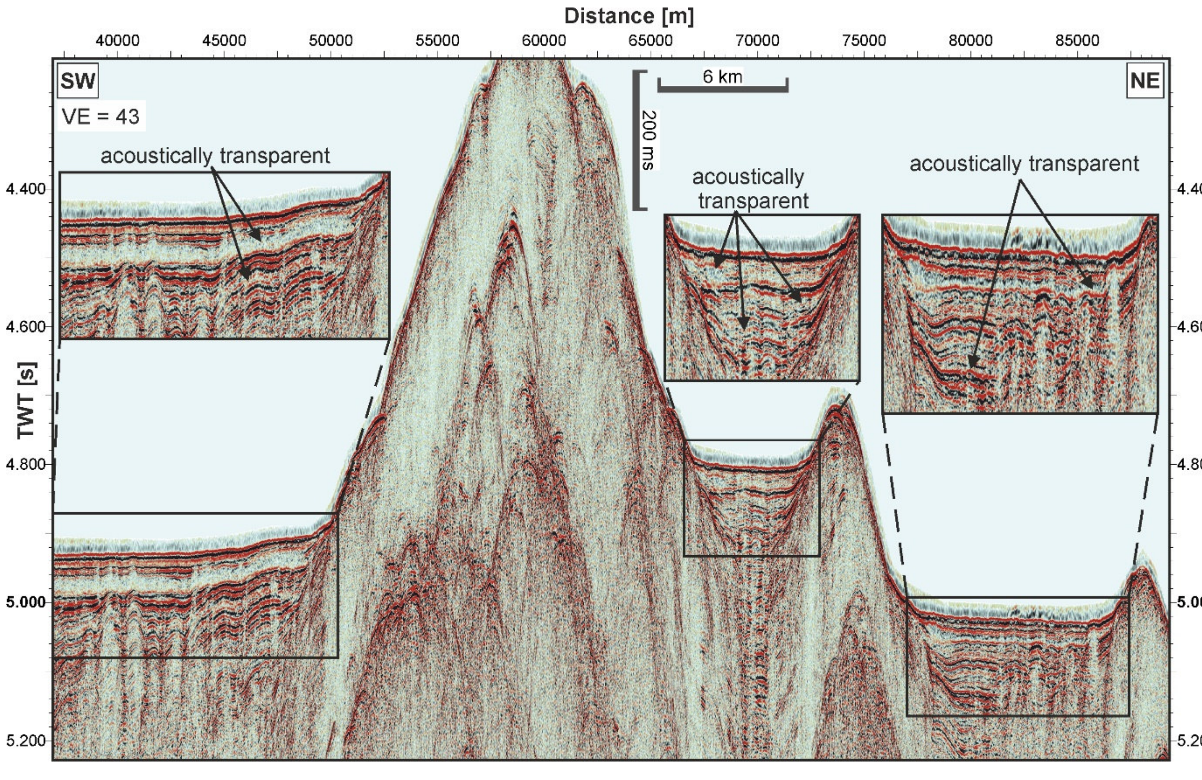

Fig. 5.6 Part of profile 4001 northwest of the Aegir Ridge. The profile runs from southwest to northeast and crosses three sedimentary infill structures separated by bathymetric highs. For location see Fig. 5.4.

Figure 5.6 shows a part of profile 4001 located northwest of the Aegir Ridge. A major bathymetric high separates a sedimentary infill structure in the southwest from two sedimentary infill structures in the northeast which in turn are separated by another bathymetric high. All three infill structures are located in different water depths and reveal slightly different seismic facies.

The northernmost infill structure is the lowest one and shows a varying sediment infill. The continuous infill varies in the lower part laterally from horizontal reflections in the southwest to wavy reflections in the northeast. The upper part is laterally uniform. In addition, the infill seems to onlap at both flanks. However, the seismic reflections are generally high-amplitude while at least two acoustically transparent layers are observable that may indicate turbidites. The infill structure in the middle is bounded by both bathymetric highs. It is both the shallowest and the narrowest of all three. The entire infill is laterally uniform and shows only differences in vertical direction. Three acoustically transparent layers can be identified that may also indicate turbidite deposits. The infilling is generally characterised by low amplitudes with a few intercalated high-amplitude reflections.

The seismic characteristics of the southernmost infill structure are comparable to the northernmost one. Towards the flank of the bathymetric high the reflections in the lower part are wavy and onlap the high. At c. 40,000 m distance two anticlinal features emerge into the overlying strata. However, the lower high-amplitude unit is intermitted by a thin acoustically transparent layer that indicates a turbidite deposit. The upper unit is mainly characterised by a thick acoustically transparent package indicating a major turbidite. This turbidite is overlain by high-amplitude reflections that finish the infilling.

5.1.3 Results German Bight - glaciogenic complex

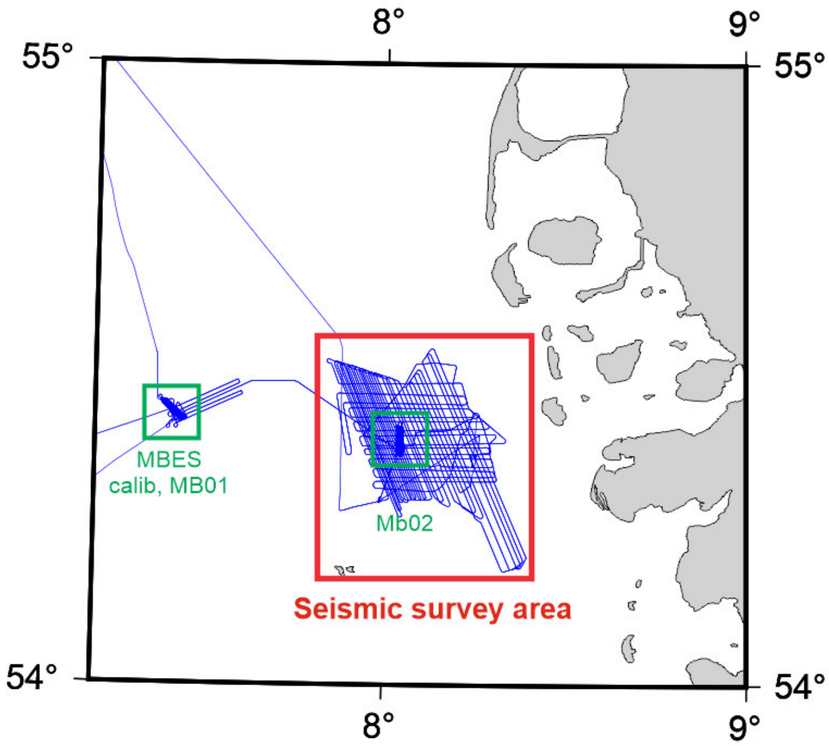

Fig. 5.7 Overview and track chart map of the second working area in the German Bight with main focus on a very dense grid with seismic survey lines (red rectangle) sailed with only 400 meters profile distances. In addition, dedicated multibeam surveys were performed (green rectangles) to resolve peculiar depressions found on the seabed with high resolution and multispectral MBES.

After the transit from Norway towards the German Bight we were able to start our seismo-acoustic work program again on the morning of February 12th in sunshine and calm seas near Heligoland, where glaciations have left deep buried valleys and other traces of ice sheets in the subsurface. Northeast of Heligoland, the so-called Heligoland glaciotectonic complex (HGC) has been found in the shallow subsurface that likely dates back to the Elsterian glaciation or earlier. The HGC extends over 660 km^2 and is thus one of the largest of its kind (Lohrberg et al., 2020). It consists of glaciotectonically thrusted Plio- and Pleistocene sediments in depths of about 40 to 250 m below the current seafloor. A shift from disturbed Quaternary strata to undisturbed Miocene strata is marked by a flat décollement or detachment plane.

We have sailed 60 profiles summing up to approx. 1600 km of 2D high-resolution seismic profiles. A preliminary data analysis shows that we can well identify thrust sheets, thrust faults, anticlines and the known décollement (Fig. 5.8). A first approximation of the thrust direction confirms previous findings (Lohrberg et al., 2020, 2021). Tunnel valleys incised through the thrust sheets and subsequently filled are visible on most profiles. Sporadically, smaller near-surface channels were identified in the data. However, the preliminary data also show the artefacts to be expected in shallow water, namely the multiple reflections of both the seafloor and deeper interfaces. A special processing will be needed to suppress these artefacts to provide the data in publication-grade quality.

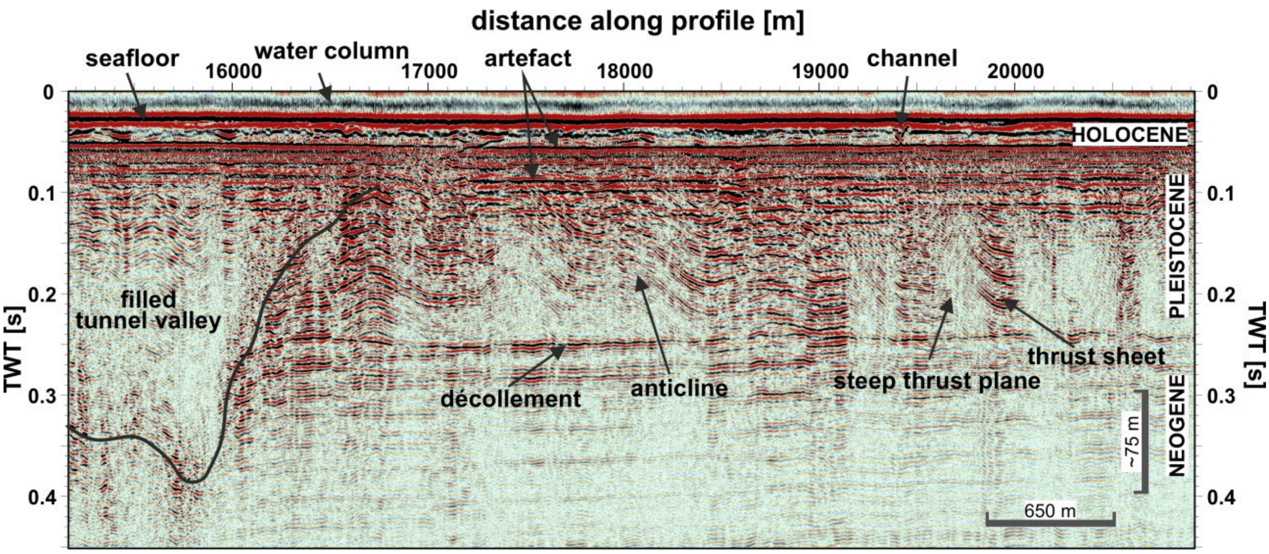

Fig. 5.8 Seismic profile in the west of the working area. To the NNW, a large subglacial meltwater channel (tunnel valley) is visible, which cuts the SSE located thrust sheets. The sheets "rise" from a very shallow and slightly NNW-dipping décollement. From SSE to NNW, the steep sheets progressively transition into flatter sheets and folds. These glacial landforms are underlain by Neogene sediments, which are thus quasi undisturbed.

Our dense survey grid targeted the HGC to close gaps in previous data and to facilitate the interpretation and reconstruction of thrust faults. The high vertical and horizontal resolution of this new data set in combination with data from AL496 will result in a net line spacing of just 400 m, which will suffice to map single thrust sheets, which display lengths of 400 m and longer. The denser grid will also be used to refine and to extend the distribution of tunnel valleys in the area (Lohrberg et al., 2020). Additional profiles aligned with the base of the tunnel valleys will likely give additional insights on the origin and fill of the tunnel valleys. All of these information will be essential for further investigations of the aquifer potential of tunnel valleys and to refine our knowledge about the Pleistocene stratigraphy of the southeastern North Sea.

5.2 Multibeam bathymetry

(J. Schneider von Deimling)

5.2.1 Systems overview and installation

Hull mounted systems EM122 and EM712, and moonpool mounted NORBIT iWBMS

Bathymetric data collection during MSM98/2 was conducted with three different Mill-Cross multibeam echsosounder systems. The two hull-mounted MBES Kongsberg systems EM122 and EM712 are protected by an ice shield window. In addition, we installed our NORBIT shallow water iWBMS multibeam sounder in the moonpool of R/V MERIAN for multifrequency seafloor analyses surveying.

The EM122 operates with frequencies between 10.5 and 13.5 kHz to code different sectors. On RV MARIA S. MERIAN, the EM122 transducers are 4 m by 4 m long thus providing an angular beam resolution of 2 ° by 2 ° and full ocean depth range. The EM712 on R/V MERIAN has 0.5 x 0.5° RX/TX transducers and is mainly operated with FM chirp between 70-100 kHz, but can also be run with frequencies as low as 40 kHz. Dual-ping mode, where one beam is slightly tilted forward and the second ping slightly tilted towards the aft of the vessel, was frequently used to increase sounding density.

Our NORBIT iWBMS chirp multibeam system was operated in a frequency range between 150-410 kHz in multispectral mode with receiver picking 80 kHz wide bands around around 190 kHz and 370 kHz, repspectively, using a 1x1° array. We ran a prototype firmware kindly provided by NORBIT allowing us to acquire two frequencies at the same time through matched filtering for 190 and 370 kHz, respectively. This special setup limited the opening angle from 150° in single frequency chirp mode to 130° in multispectral mode for technical restrictions reasons. To keep the data consistent and to keep backscatter comparable throughout each survey we fixed the pulse length, gains, and filter setting in the beginning of each working area.

An AML C-keel velocity probe is mounted next to the moonpool of R/V Merian some meters apart from the transducers. Motion, heading, position, and timing are provided by a Kongsberg Seapath 320 system and transmitted to the Processing Unit (PU) in real time. For vertical sound velocity profiling we deployed an AML probe as well as released several XSVs manufactured by Lockheed Martin in deeper water (Fig. 5.11). To deal with tidal seawater variations and river runoff dynamics we plotted the thermo-salinographic data in real-time in the ships database WERUM system to monitor sudden changes in temperature and salinity (Fig. 5.12). Tidal height reduction was not performed online but will be corrected in postprocessing by backward model data kindly provided by the German federal hydrographic agency (BSH).

The Kongsberg systems were motion-compensated by the onboard Seapath 320 system. In addition we locked binary Seapath format id #26 data projected into the moonpool plate were our NORBIT MBES was installed. Part of the surveying was performed in very shallow water < 20 m in the German Bight, therefore, we also logged Seapath real heave data (.srh) to correct for heave in postprocessing.
The NORBIT offset were determined by means of the Parker report and manually adapted with offsets between sonar head and primary antenna on the first deck given in Table 5.1. However, the applanix motions sensor heading alignment failed to calibrate possibly associated with errorneous offsets in Table 5.1. We connected the native NORBIT recording software to the onbord internet and received RTK GPS corrections kindly provided by AXIONet via the NTRIP protocol and achieved GPS RTK FIX status. Offset reconstruction may be possible by postprocessing the data with POSPAC.

Tab. 5.1 Installation offsets required for the CAU NORBIT multibeam system to run on R/V Merian.

<u>Offsets</u> [m]
Our relative coordinate reference system is:
positive X forward
positive Y starbord
positive Z upward

	X	Y	Z
Fix Point 35	-13,472	+2,301	+10,134
Center of the moonpool plate engaged	+3,57	+0,881	-7,789
Antenne Stb	-14,002	+1,201	+9,2422

Norbit (mounted below moonpool plate with pole and POM ring):
Positive X foward
positive Y starbord
positive Z downward

	X	Y	Z
Center of the moonpoolplate is engaged	-0,3057	+0,0083	-0,554
Antenne Stb	-17,878	+0,328	-17,585
MRU	-3,876	-0,889	-8,343

Fig. 5.9 Installed antenna on the handrail, yellow deck.

5.2.2 Processing

We ran calibration lines for all three multibeam systems. E.g. a full patch test was sailed on 26.01.2021 for EM712 at a “wreck site” 22 nm northwest of the Island Heligoland. We revisited the wreck site in the mid of February to perform a full patch test here for our NORBIT iWBMS. In between the EM122 was roll calibrated in deeper waters off the continental Norwegian margin with a roll deviation of only EM122 Roll offset +0.021°.

Data were analysed in MBSystem, Qimera, and FMGT. We loaded dedicated sound velocity profiles, and applied the roll offset. Finally the multibeam data were medium spline filtered in Qimera and exported as .gsf for backscatter inspections in the QPS software FMGT and visualized partly in GMT.

The EM122 performed without any troubles during the cruise and delivered good data even during very rough sea states. The bathymetry from the Tampen headwall towards Aegir ridge plots smooth and featureless. The Aegir ridge itself appears very pronounced, with flanks as shallow as 2200 m, the maximum ridge through depth in the surveyed area was found around 3800 m with a trend of slight deepening towards southwest. The morphology within the through plots very hummocky with structures several hundred meters large and ~50 m high which we partly interpreted as local slope failures within the ridge itsself. This inhomogeneity is also reflected in the backscatter gathered from the EM122 (not shown).
Close to the southeasterly start of the cross section profile in Fig. 5.10 a gate into the ridge can be identified possibly allowing for direct sediment transport into the through.

5.2.3 Results Tampen

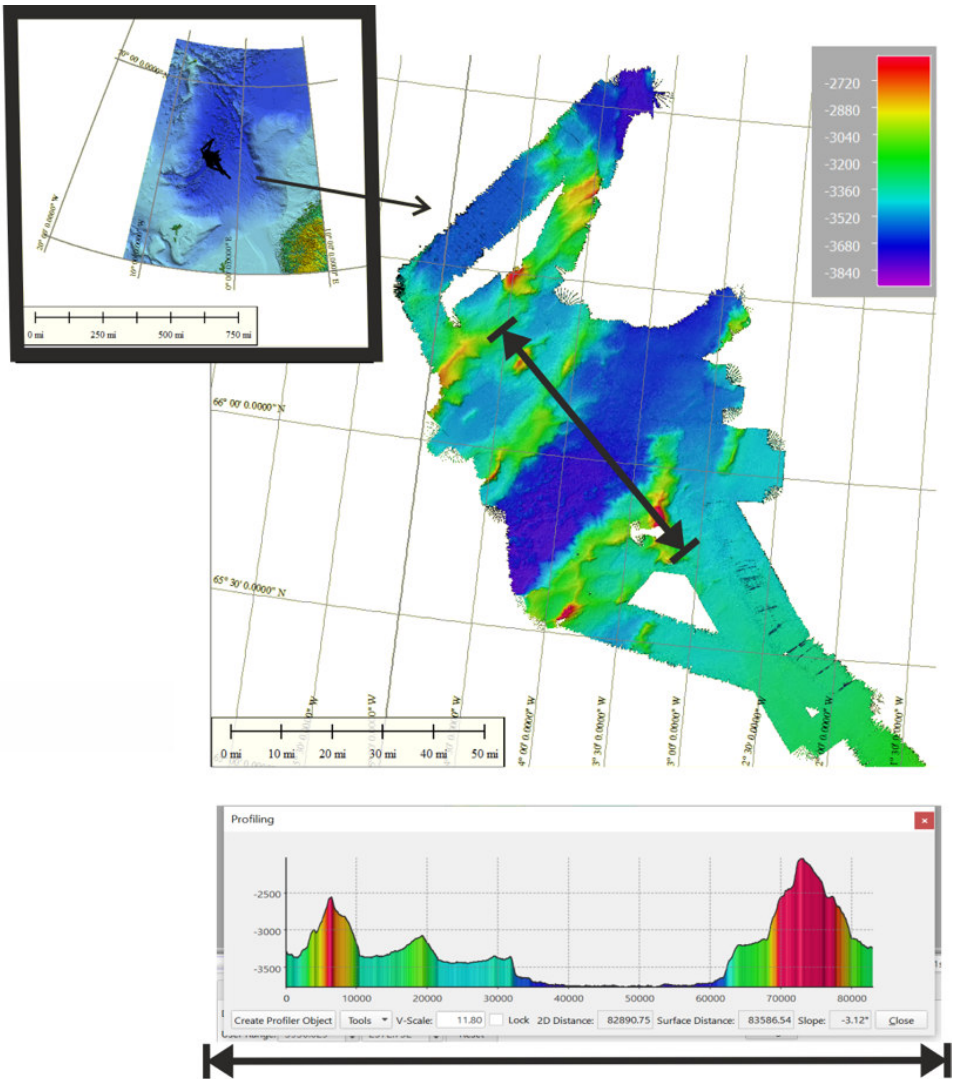

Fig. 5.10 Overview map showing the area covered with both, multibeam and subbottom profiling across Aegir ridge during MSM98/2 (Projection UTM 32 N).

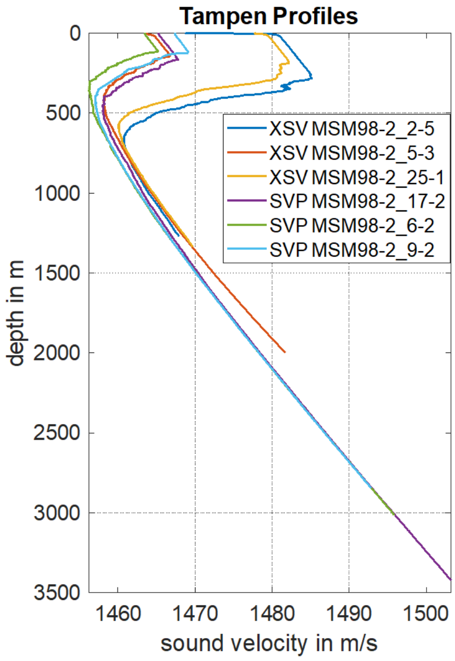

Fig. 5.11 Sound velocity profiles taken off Norway with both, underway XSVs and stationary SVPs until 2000 m. Depth was extrapolated according to the pressure dependency of sound velocity.

5.2.4 Results German Bight

The German Bight was surveyed with the hull mounted KONGSBERG EM712 and our moonpool mounted iWBMS NORBIT multibeam. The German Bight is a challenging area for accurate shallow water MBES surveying given its high tidal dynamics causing pronounced spatio-temporal water level and sound velocity changes, complex tidal fronts, wind driven water level fluctuations, and strong currents causing possibly issues (Fig. 5.12).

The EM712 performed not without problems in shallow water. Especially when ping rates were high and water column records were switched on the system sometimes hung up. The NORBIT MBES ran smoothly throughout the surveying, however, our Applanix Wavemaster motion sensor failed to initialize the heading, likely due to inaccuracies in static offsets between primary antenna and the sonar head lowered in the moonpool of Merian for the first time. The errors might be recoverable in postprocessing of the motion sensor data that have all been logged in full sample speed in the Applanix raw data format.

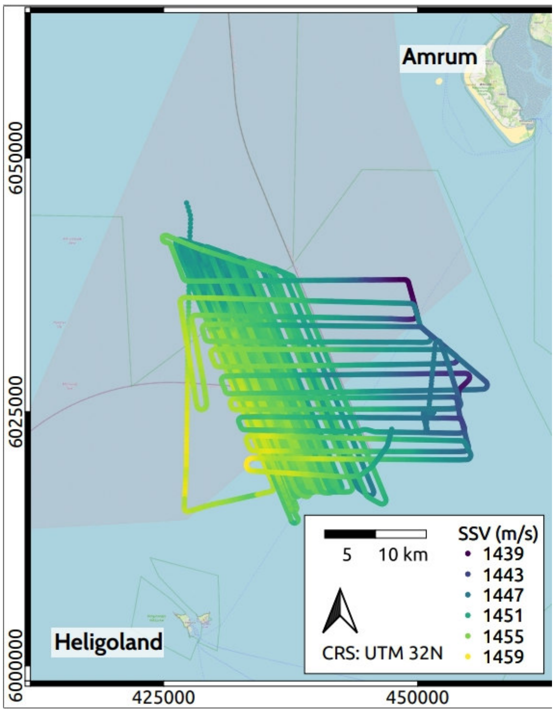

Fig. 5.12 Plot showing the complex sea surface sound velocity distribution derived from the MERIAN onboard thermosalinograph realtime system.Water insuction appears on the hull in appr. 6.2-6.8 m water depth.

We ran the MBES systems in two operating modes. On the one hand EM712 was logged together with the streamer seismics and subbottom profile to complement the seismic survey outlined in Fig. 5.7 (red triangle). Herewith, we occasionally switched on water column imaging to detect possible seepage. No coverage in between the lines was achieved, though, bathymetric features like irregular depression and some sorted bedforms partly emerge. Nevertheless, we did not identify morphological or backscatter anomalies that can be correlated to the targeted shallow channel and tunnel valley systems visible in Parasound and streamer seismic sections.

On the other hand dedicated MBES surveys were sailed with lines narrow enough to obtain full coverage (Fig. 5.7 green rectangle). As reported earlier (Krämer et al., 2017) we found hundreds of 10-30 cm deep depressions. We find their appearance to be atypical with ring-shaped depressions spanning a few meters on sandy seafloor, often characterized by concentric highs and irregularly buckled rims , and the majority of them only 0.1m deep (Fig. 5.13). Some occur in a horseshoe shape, and are accompanied by backscattering anomalies. None of those characteristics have been reported for pockmarks so far. As a working hypothesis we attribute their origin to benthic feeding of harbor porpoise, the most abundant cetacean species in the North Sea.

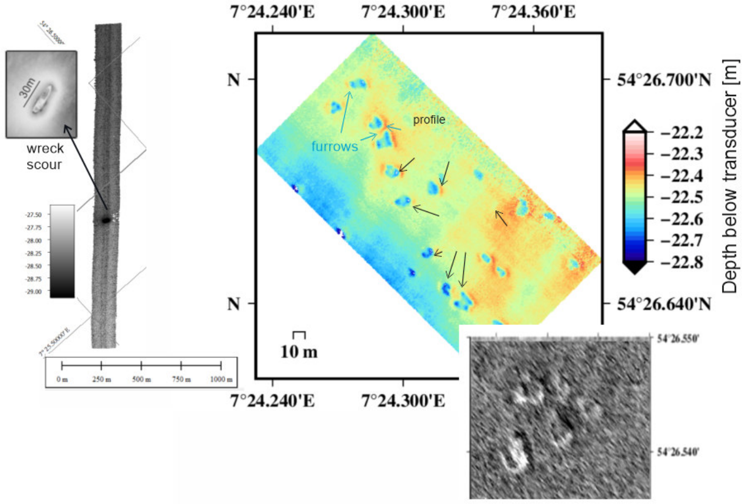

Fig. 5.13 Left: B/W bathymetric map showing the patch test calibration survey lines ran over the wreck site described in Krämer et al. (2017) and Karstens (2018) with hundreds of depressions and a few scours, especially around the wreck itself. Right: close up view disclosing the depressions and their enigmatic shape and snippet backscatter. Note the bathymetric chart shows ungridded point cloud data derived from our NORBIT broadband chirp MBES.

5.3 Subbottom profiling

(A. Lohrberg, J. Schneider von Deimling, K.-F. Lenz, H. Grob)

5.3.1 System overview and processing

The PARASOUND System DS3 (P70) installed on R/V Merian is a parametric echo sounder manufactured by TELEDYNE ATLAS HYDROGRAPHIC GmbH. The transducer transmits signals with 70 kW transmission power to enable a maximum penetration depth of up to 150 m in soft sediments. The system uses the parametric effect that occurs when very high sound waves of similar frequencies are generated simultaneously, where the sum and the difference frequencies are generated, although with much lower intensities. For the PARASOUND System on MARIA S. MERIAN, 19.3 kHz is the fixed Primary Low Frequency (PLF) that distributes energy within a beam of ~4.5°. The second primary frequency (Primary High Frequency, PHF) can be varied between 18 kHz to 24 kHz, resulting in a range of frequencies from 0.5 to 7.0 kHz. The SLF signal travels within the narrow 19.3 kHz beam, which is much narrower than e.g. the 30° beam of a 4 kHz signal when emitted directly from the same transducer. Therefore, a higher lateral resolution can be achieved with a relatively small transducer, and imaging of small-scale structures on the seafloor is superior to conventional systems.

The PARASOUND System supports different ping modes – quasi-equidistant, pulse train, transmission on request and single pulse mode. In the transmission on request mode the active period (ping rate) is controlled by Kongsberg's Synchronizing Unit K-Sync, a trigger box, to avoid interferences when different systems are running. In shallow water with EM712 we surveyed using the trigger box. Towards the Tampen area and in the Aegir ridge the EM122 was used because of higher water depth. Therefore, there were no interferences with the PARASOUND and thus the K-sync trigger box was not used. The system was operated with a maximum transmission voltage of 160V. In the TAMPEN area the system was operated in quasi-equidistant mode (with multiple pulses in the water column). The PARASOUND System was operated almost continuously in both working areas of cruise MSM 98/2, but had to be turned off during transit times in Danish and Norwegian waters.

In both working areas the Secondary Low Frequency (SLF) was set to 4 kHz. In both areas the pulse type was chosen to be continuous wave. Both SLF and PHF were stored as ASD files, and additionally in PS3 and SGY format using the carrier Frequency mode. The PHF signal was only used for seafloor detection. The PS3 SLF data (4 kHz) was then converted to *.sgy-files using the ps32sgy tool (written by Hanno Keil, University of Bremen). The software allows for a frequency filtering (used parameters: low cut 2 kHz, high cut 6 kHz, 1 iteration) and the subtraction of a mean value. Afterwards the sgy-data was imported into IHS Kingdom® for visualization and quality control.

5.3.2 Preliminary results Tampen slide and Aegir ridge

The PARASOUND surveys where mainly used as a reconnaissance survey for the gravity cores in the Tampen working area. It was essential to find locations were chances were given to reach older sedimentary material with our 10 m long gravity core. To achieve this we concentrated on possible pitchout areas at the flanks of valleys, or even at adjacent valleys further up as possible sedimentation regime of any turbidite. Parasound performed without significant problems and we were able to find older laminated strata on the volcanic ridge

Fig. 5.14 shows a part of the Aegir ridge west of Norway in more than 3500 m water depth. Stratified layers in the upper part alternate with chaotic to transparent layers getting thicker with the depth. Two gravity core locations are marked to find a sediment layer to detect the Tampen slide for a correlation with the turbidites and to verify the thesis that the Tampen slide is much younger than we reported before.

Fig. 5.14 Sediment echo sounder data from the Aegir ridge off Norway: Red lines indicate the location of

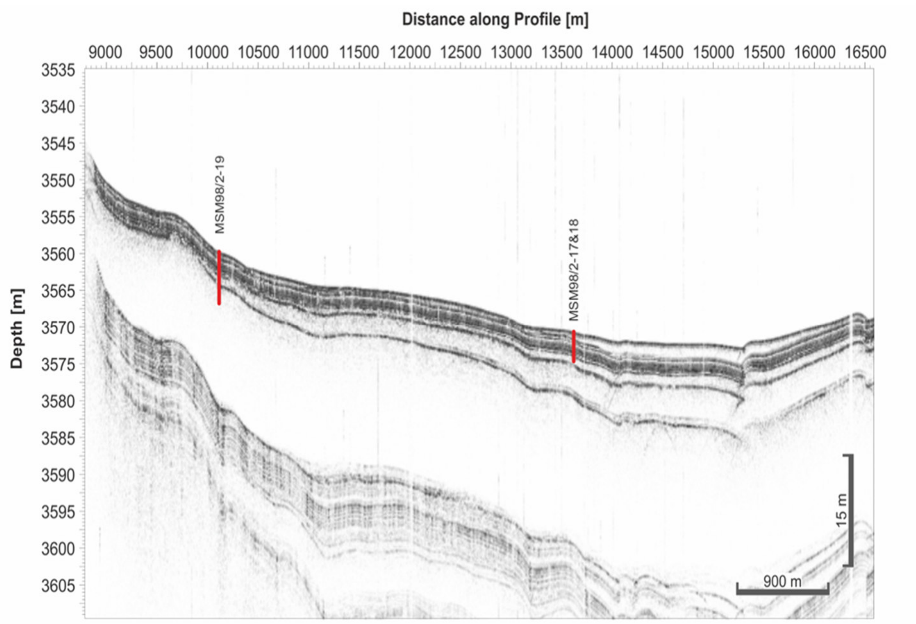

gravity cores MSM98/2-17&18 and MSM98/2-19

5.3.3 Preliminary results Heligoland glaciogenic complex

In the second working area the transmission on request mode was used to synchronize the PARASOUND pings with the EM712 pings to avoid interference in shallow water (ping synchronization rate 1:7).

Unfortunately, the system failed on the 13th of February in the early morning because of a shortage in power supply. A new power supply unit was installed. Next day it failed again because of issues with the synchronized trigger rate, after restart and adjustment of the ping synchronization rate to 1:11 there were no further problems until the end of the cruise.
At first, the system was operated with 60 V. On the 13.02.2021 the transmission voltage was adjusted to 120 V and on the 14.02.2021 to 160 V to achieve a higher penetration. Furthermore, different pulse types were tested first, but a frequency modulated pulse type (chirp) showed inferior results. Thus, the rest of the survey was conducted using the continuous wave mode again.

Some first results of the sediment echo sounder data from the HELGLA working area are shown in the following section. In the shallow waters of the German bight the PARASOUND system was generally able to image the subsurface up to depth of ~10m. Below that S/N diminished and seafloor multiples strongly hider interpretation of the records.

The first example (Fig. 5.15) images a filled former river bed (distance along profile ~3700-4000 m) located around 54°17.703 N, 007°59.218 E. The structure is incised into a transparent material and overlain by a thin also transparent layer, interpreted as the mobile North Sea sands. The infill of the riverbed is well stratified and the eastern bank features prominent terrace structures. Within the transparent material underlying the river structure further reflectors are visible, indicating multiple phases of deposition and erosion. Below ~0.042 s TWT the seafloor and also reflector multiples hinder interpretation. This profile was recorded using a transmission voltage of 60 V.

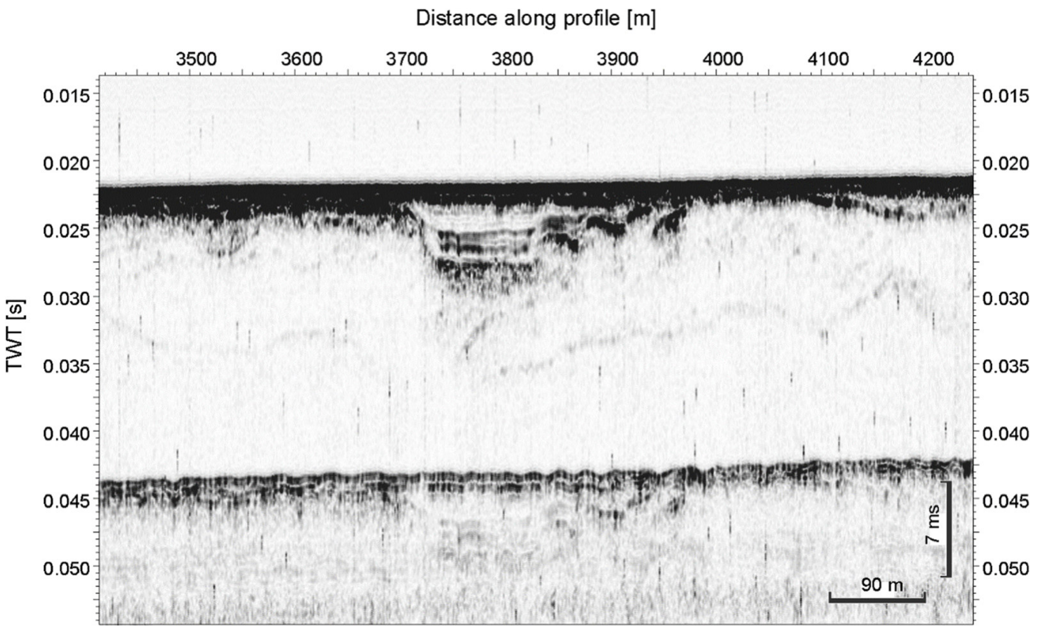

Fig. 5.15 Sediment echo sounder data from 54°17.703 N, 007°59.218 E.

The second example profile (Fig. 5.16) shown below was recorded around 54°19.375 N, 008°08.048 E. The uppermost layer is transparent, varies in thickness and is interpreted as the mobile North Sea sands. Below the mobile sand layer the profile features different characteristics in the left and right half, respectively. The left half shows two transparent units separated by an undulating reflector. The upper unit features clinoforms. The right half is dominated by well-stratified units. Channel river structures incised in the stratified units as well as the transparent "basement" indicate a succession of cut and fill mechanisms. Below ~0.030 s TWT multiples hinder interpretation. This profile was recorded using a transmission voltage of 160 V.

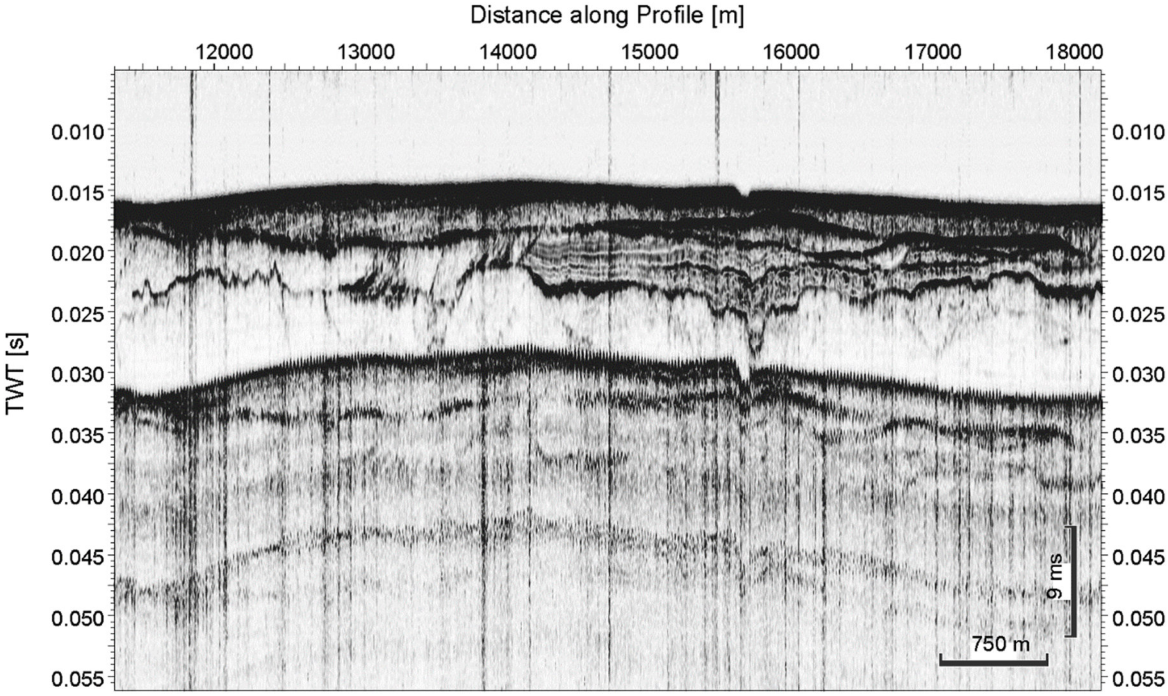

Fig. 5.16 Sediment echo sounder data example from the German Bight HCG area.

5.4 Sediment sampling

(K.-F. Lenz, J. Scheffler, R. Barret)

5.4.1. Gravity coring

A gravity corer with a weight of 1.8 tons and a core barrel length of 10 m (2x 5m) was used to recover long sediment sequences. The gravity corer was lowered into the sediments with a speed between 1 and 1.5 m/s depending on the expectations based on the subbottom profiler data. Unfortunately, an exact positioning of the gravity corer was not possible, because the USBL system was not working. Hand-drawn lines ("*Bleil-Linie*") along the plastic liners were used to retain the orientation of the core. Once on board, the sediment core was cut into 1-m-sections, closed with caps (yellow at the top and transparent at the bottom) and labelled according to a standard scheme (Fig. 5.17). The gravity corer was used at 7 stations in working area one at the Aegir Ridge. All coring attempts were successful with sediment recoveries between 4.52 and 7.50 m resulting in total core recovery of ~ 41 m. Unfortunately, the gravity corer did not penetrate into the seafloor at 1 station in working area two in the German Bight due to a sand layer at the surface. Two coring attempts were unsuccessful with no recovery.

All recovered cores were cut lengthwise and divided into an archive and a work half. The archive half was used for core photography and the work half was used for a visual core description. No subsampling was done. The core half’s were stored in D-tubes for transportation in the scientific freezer at 5°C.

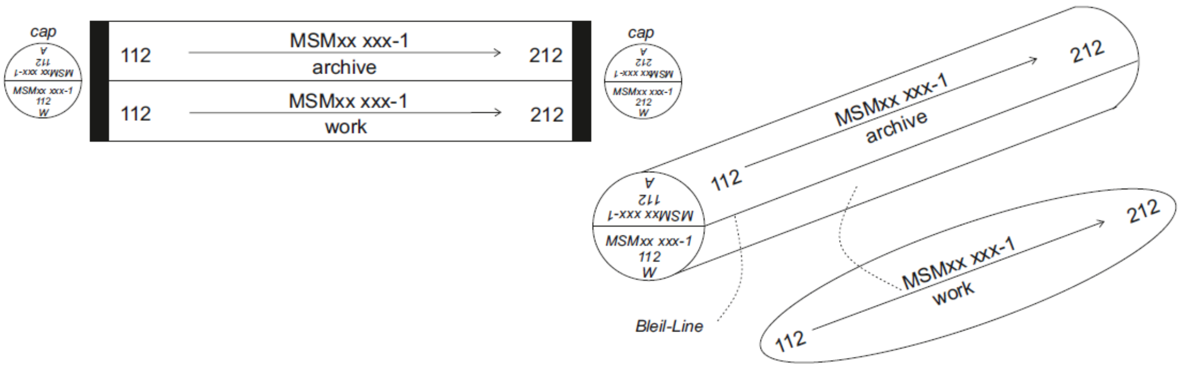

Fig. 5.17 The sediment cores were cut into 1-m-sections, closed with caps (yellow at the top and transparent at the bottom) and labelled according to a standard scheme.

Tab. 5.2 List of gravity cores retrieved during R/V MARIA S. MERIAN Cruise MSM98/2.

Station No	Gear	Latitude	Longitude	Water Depth	Recovery	Remarks
		(°)	(°)	(m)	(cm)	
MSM98/2_6	GC 10	65° 35.03’ N	003° 57.18’ W	3119	630	
MSM98/2_7	GC 10	65° 35.15’ N	003° 57.23’ W	3118	649	~ 15 cm of sediments at the top in a plastic bag
MSM98/2_9	GC 10	65° 58.81’ N	002° 40.22’ W	3413	452	
MSM98/2_11	GC 10	65° 58.79’ N	003° 25.62’ W	3648	615	
MSM98/2_17	GC 10	66° 06.23’ N	004° 42.43’ W	3526	503	
MSM98/2_18	GC 10	66° 06.23’ N	004° 42.43’ W	3530	503	~ 4 cm of sediments at the top a plastic bag
MSM98/2_19	GC 10	66° 04.84’ N	004° 45.58’ W	3519	750	
MSM98/2_29-1	GC 5	54° 17.70’ N	007° 59.25’ E	21.9	-	No penetration
MSM98/2_29-2	GC 5	54° 17.69’ N	007° 59.21’ E	21.9	-	No penetration

A visual core description was carried out after splitting the cores. This description summarizes the findings of a first core analysis like grain size, colour, main components, structures and layer boundaries. A NICON D5100 Camera was used to take high-resolution photographs of the archive halves of the cores. The camera was mounted on a frame with two lights and a scale to ensure same condition for every photo. The photographs allow a detailed graphical analysis of the cores beyond the visual core description done in the lab.

Preliminary visual analysis of the seven sediment cores collected in the Aegir Ridge indicates the presence of at least four significant turbidite layers (up to 3.5 m thick) and a ~2 m thick, blocky debris flow. Photographs of these cores are included in the Appendix. Core MSM98/2-11 (Fig. 5.18) was collected on the southern side of the Aegir Ridge and contains two significant mass wasting deposits – (i) a two-metre thick, muddy, grey unit characteristic of turbidites in the upper part of the core; and (ii) a clast-containing (cm-to-dm scale), sandy (mixed grain size), 2 m-thick layer at the base of the core, which is characteristic of debris flows. Layer X, a distinctive ~10 cm thick silty-clay layer present in all of the MSM98/2 cores, is also clearly evident in core MSM98/2-11, and will be useful for correlating the sedimentary stratigraphy across the collected cores.

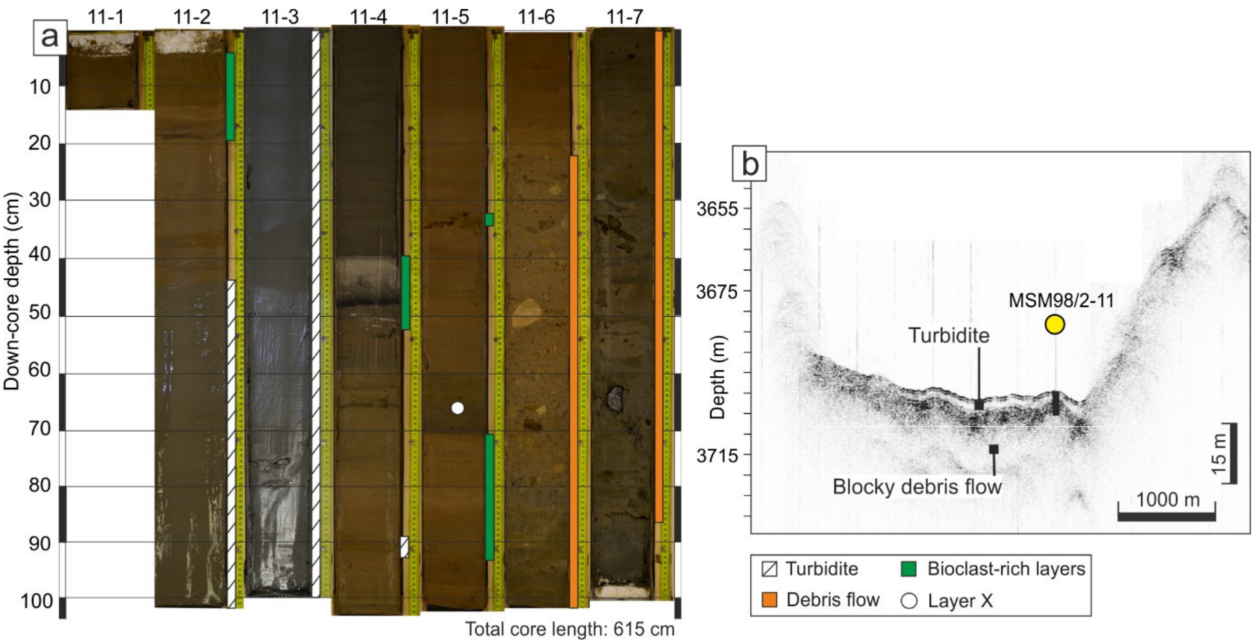

Fig. 5.18 (a) Photographs and preliminary interpretation of core MSM98/2-11. Layer X: a distinctive ~10 cm thick silty-clay layer present in all of the MSM98/2 cores. (b) Parasound profile crossing the site where MSM98/2-11 was cored.

5.4.2 Grab Sampling

Van Veen grab sampling was performed eight times in the German Bight at seven stations to recover surface samples. The locations for sampling were chosen based on the backscatter data recorded with the NORBIT Echosounder. A HELCOM grab sampler was used, which penetrate into the seafloor with its own weight. During sampling the sediments get disturbed. The recovered samples were described and photographed on board. They are used to validate the acquired data of the performed hydroacoustic survey. Further, two samples (size of sampling box 11cm x 7cm x 4cm) of every grab were taken for further laboratory analysis. The samples were stored at -20°C.

Tab. 5.3 Positions of Grab samples in the German Bight

Station No	Gear	Latitude	Longitude	Water Depth
		(°)	(°)	(m)
MSM98/2_37-1	GS	54° 24.53’ N	008° 00.74’ E	19.0
MSM98/2_37-2	GS	54° 24.53’ N	008° 00.74’ E	19.0
MSM98/2_38-1	GS	54° 24.53’ N	008° 02.73’ E	19.3
MSM98/2_39-1	GS	54° 23.14’ N	008° 02.85’ E	19.3
MSM98/2_40-1	GS	54° 22.56’ N	008° 02.95’ E	18.5
MSM98/2_48-1	GS	54° 26.72’ N	007° 24.28’ E	29.2
MSM98/2_49-1	GS	54° 26.72’ N	007° 24.28’ E	29.3
MSM98/2_50-1	GS	54 ° 25.25’ N	007° 25.32’ E	28.5

6 Ship’s Meteorological Station

There was no meteorologist on board during the cruise.

7 Station List MSM98/2

Tab. 7.1 Station list

Station ID No.	Date / Time [UTC]	Device	Action	Latitude	Longitude	Depth [m]
MSM98/2_1-1	26.01.2021 17:02	EM712 Shallow-water Multibeam Echosounder	profile start	54° 26,017' N	007° 25,558' E	28,8
MSM98/2_2-1	28.01.2021 12:12	Seismic Towed Receiver	Streamer in water	62° 59,923' N	001° 09,827' E	1139
MSM98/2_2-2	28.01.2021 16:52	Seismic Source	profile start	63° 04,699' N	001° 01,597' E	1251,3
MSM98/2_2-3	28.01.2021 16:52	EM122 Deep-Sea Multibeam Echosounder	profile start	63° 04,737' N	001° 01,554' E	1248,7
MSM98/2_2-4	28.01.2021 16:52	Parasound P70	profile start	63° 04,738' N	001° 01,553' E	1248,7
MSM98/2_2-5	28.01.2021 18:55	Expendable Sound Velocimeter	in the water	63° 12,088' N	000° 53,621' E	1422,7
MSM98/2_3-1	30.01.2021 05:59	Seismic Towed Receiver	Streamer in water	64° 35,148' N	000° 13,290' W	2669,2
MSM98/2_3-2	30.01.2021 06:14	Seismic Source	Airgun in water	64° 35,782' N	000° 13,496' W	2675,5
MSM98/2_3-3	30.01.2021 06:45	EM122 Deep-Sea Multibeam Echosounder	profile start	64° 37,405' N	000° 13,987' W	2693,5
MSM98/2_3-4	30.01.2021 06:45	Parasound P70	profile start	64° 37,428' N	000° 13,994' W	2698,3
MSM98/2_4-1	30.01.2021 22:27	EM122 Deep-Sea Multibeam Echosounder	profile start	65° 23,859' N	001° 58,336' W	3174,5
MSM98/2_4-2	30.01.2021 22:27	Parasound P70	profile start	65° 23,859' N	001° 58,336' W	3174,5
MSM98/2_5-1	31.01.2021 05:15	EM122 Deep-Sea Multibeam Echosounder	profile start	65° 35,929' N	004° 05,913' W	2928,1
MSM98/2_5-2	31.01.2021 05:15	Parasound P70	profile start	65° 35,959' N	004° 05,929' W	2927,9
MSM98/2_5-3	31.01.2021 07:21	Expendable Sound Velocimeter	in the water	65° 47,830' N	004° 11,018' W	3736,1
MSM98/2_6-2	01.02.2021 14:31	Sound Velocity Profiler	max depth/on ground	65° 35,029' N	003° 57,179' W	3122,6
MSM98/2_6-1	01.02.2021 14:31	Gravity Corer	max depth/on ground	65° 35,030' N	003° 57,179' W	3117
MSM98/2_7-1	01.02.2021 16:54	Gravity Corer	max depth/on ground	65° 35,152' N	003° 57,234' W	3116,6

MSM98/2_8-1	01.02.2021 17:55	EM122 Deep-Sea Multibeam Echosounder	profile start	65° 35,185' N	003° 57,037' W	3116,6
MSM98/2_8-2	01.02.2021 17:55	Parasound P70	profile start	65° 35,176' N	003° 56,969' W	3117,5
MSM98/2_9-1	02.02.2021 09:06	Gravity Corer	max depth/on ground	65° 58,808' N	002° 40,224' W	3413
MSM98/2_9-2	02.02.2021 09:06	Sound Velocity Profiler	max depth/on ground	65° 58,808' N	002° 40,224' W	3413
MSM98/2_10-1	02.02.2021 11:51	EM122 Deep-Sea Multibeam Echosounder	profile start	65° 57,418' N	003° 28,895' W	3658,9
MSM98/2_10-2	02.02.2021 11:51	Parasound P70	profile start	65° 57,418' N	003° 28,895' W	3658,9
MSM98/2_11-1	02.02.2021 14:23	Gravity Corer	max depth/on ground	65° 58,795' N	003° 25,617' W	3650
MSM98/2_12-1	02.02.2021 19:40	Seismic Towed Receiver	Streamer in water	65° 15,480' N	002° 08,421' W	3149
MSM98/2_12-2	02.02.2021 20:18	Seismic Source	profile start	65° 16,891' N	002° 04,313' W	3159,1
MSM98/2_12-3	02.02.2021 20:18	EM122 Deep-Sea Multibeam Echosounder	profile start	65° 16,891' N	002° 04,311' W	3153,9
MSM98/2_12-4	02.02.2021 20:18	Parasound P70	profile start	65° 16,892' N	002° 04,308' W	3153,9
MSM98/2_13-1	03.02.2021 13:53	Seismic Towed Receiver	Streamer in water	65° 54,658' N	003° 07,821' W	3429,1
MSM98/2_13-2	03.02.2021 14:08	Seismic Source	Airgun in water	65° 55,175' N	003° 06,074' W	3417,8
MSM98/2_13-3	03.02.2021 15:00	EM122 Deep-Sea Multibeam Echosounder	profile start	65° 57,422' N	002° 59,592' W	3465,4
MSM98/2_13-4	03.02.2021 15:01	Parasound P70	profile start	65° 57,464' N	002° 59,642' W	3458,7
MSM98/2_14-1	03.02.2021 17:43	Multibeam	profile start	66° 03,448' N	003° 25,112' W	3577,7
MSM98/2_14-2	03.02.2021 17:43	Parasound P70	profile start	66° 03,472' N	003° 25,169' W	3606,9
MSM98/2_15-1	04.02.2021 11:42	Seismic Towed Receiver	Streamer in water	66° 28,482' N	002° 53,305' W	3633,2
MSM98/2_15-2	04.02.2021 11:54	Seismic Source	Airgun in water	66° 28,056' N	002° 55,171' W	3472
MSM98/2_15-3	04.02.2021 12:31	Parasound P70	profile start	66° 26,605' N	003° 01,463' W	3662,5
MSM98/2_15-4	04.02.2021 15:52	EM122 Deep-Sea Multibeam Echosounder	profile start	66° 14,312' N	003° 28,590' W	3698,2
MSM98/2_16-1	04.02.2021 22:32	EM122 Deep-Sea Multibeam Echosounder	profile start	65° 50,720' N	004° 22,578' W	3723,8
MSM98/2_16-2	04.02.2021 22:32	Parasound P70	profile start	65° 50,759' N	004° 22,619' W	3722,8
MSM98/2_17-1	05.02.2021 07:56	Gravity Corer	max depth/on ground	66° 06,234' N	004° 42,431' W	3524,6
MSM98/2_17-2	05.02.2021 07:56	Sound Velocity Profiler	max depth/on ground	66° 06,234' N	004° 42,430' W	3529,6
MSM98/2_18-1	05.02.2021 10:09	Gravity Corer	max depth/on ground	66° 06,235' N	004° 42,432' W	3529,5
MSM98/2_19-1	05.02.2021 12:22	Gravity Corer	max depth/on ground	66° 04,842' N	004° 45,577' W	3519
MSM98/2_20-1	05.02.2021 14:35	EM122 Deep-Sea Multibeam Echosounder	profile start	66° 19,730' N	004° 48,393' W	3098,5
MSM98/2_20-2	05.02.2021 14:35	Parasound P70	profile start	66° 19,730' N	004° 48,393' W	3098,5
MSM98/2_21-1	05.02.2021 19:32	Seismic Towed Receiver	Streamer in water	67° 03,329' N	003° 40,786' W	3740,8
MSM98/2_21-2	05.02.2021 19:43	Seismic Source	Airgun in water	67° 03,199' N	003° 42,491' W	3765,8
MSM98/2_21-4	05.02.2021 20:07	Parasound P70	profile start	67° 02,885' N	003° 46,705' W	3778
MSM98/2_21-3	05.02.2021 20:07	EM122 Deep-Sea Multibeam Echosounder	profile start	67° 02,885' N	003° 46,705' W	3778
MSM98/2_22-2	07.02.2021 11:13	Parasound P70	profile start	65° 58,654' N	003° 03,532' W	3498,7
MSM98/2_22-1	07.02.2021 11:13	EM122 Deep-Sea Multibeam Echosounder	profile start	65° 58,654' N	003° 03,532' W	3498,7

MSM98/2_23-1	07.02.2021 21:24	Seismic Towed Receiver	Streamer in water	64° 25,703' N	000° 23,558' W	2641,5
MSM98/2_23-2	07.02.2021 21:37	Seismic Source	Airgun in water	64° 25,826' N	000° 21,763' W	2644,1
MSM98/2_24-1	08.02.2021 10:04	Seismic Towed Receiver	Streamer in water	64° 24,652' N	000° 22,694' W	2634,4
MSM98/2_24-2	08.02.2021 10:18	Seismic Source	Airgun in water	64° 25,018' N	000° 20,840' W	2635,7
MSM98/2_24-3	08.02.2021 10:38	EM122 Deep-Sea Multibeam Echosounder	profile start	64° 25,620' N	000° 17,834' W	2645,7
MSM98/2_24-4	08.02.2021 10:38	Parasound P70	profile start	64° 25,629' N	000° 17,793' W	2645,1
MSM98/2_25-1	10.02.2021 08:36	Expendable Sound Velocimeter	in the water	63° 15,114' N	000° 49,657' E	1491,4
MSM98/2_25-1	10.02.2021 08:41	Expendable Sound Velocimeter	station end	63° 14,586' N	000° 50,381' E	1472,1
MSM98/2_26-1	12.02.2021 09:36	Seismic Towed Receiver	Streamer in water	54° 16,872' N	007° 53,682' E	26,7
MSM98/2_26-2	12.02.2021 09:48	Seismic Source	Airgun in water	54° 17,175' N	007° 55,362' E	25,2
MSM98/2_26-3	12.02.2021 10:28	EM712 Shallow-water Multibeam Echosounder	profile start	54° 18,308' N	008° 00,729' E	21,4
MSM98/2_26-4	12.02.2021 10:28	Parasound P70	profile start	54° 18,328' N	008° 00,716' E	21,4
MSM98/2_26-5	12.02.2021 12:41	Expendable Sound Velocimeter	in the water	54° 28,449' N	007° 53,393' E	21,5
MSM98/2_27-1	16.02.2021 12:39	Seismic Towed Receiver	Streamer in water	54° 25,865' N	008° 15,848' E	15,9
MSM98/2_27-2	16.02.2021 12:54	Seismic Source	Airgun in water	54° 24,794' N	008° 16,550' E	17,2
MSM98/2_27-4	16.02.2021 13:28	Parasound P70	profile start	54° 22,413' N	008° 17,205' E	15,5
MSM98/2_27-3	16.02.2021 13:28	EM712 Shallow-water Multibeam Echosounder	profile start	54° 22,413' N	008° 17,205' E	15,5
MSM98/2_27-5	16.02.2021 13:57	Expendable Sound Velocimeter	station end	54° 22,369' N	008° 13,028' E	19,5
MSM98/2_28-1	19.02.2021 10:31	Sound Velocity Profiler	max depth/on ground	54° 24,161' N	008° 15,700' E	15
MSM98/2_29-1	19.02.2021 12:20	Gravity Corer	max depth/on ground	54° 17,694' N	007° 59,214' E	21,8
MSM98/2_29-2	19.02.2021 12:25	Gravity Corer	max depth/on ground	54° 17,694' N	007° 59,215' E	22
MSM98/2_30-1	19.02.2021 13:36	Multibeam	profile start	54° 17,684' N	007° 59,169' E	22,5
MSM98/2_31-2	19.02.2021 15:36	EM712 Shallow-water Multibeam Echosounder	profile start	54° 22,723' N	008° 02,026' E	20,2
MSM98/2_31-1	19.02.2021 15:36	Multibeam	profile start	54° 22,740' N	008° 02,026' E	20,2
MSM98/2_31-2	19.02.2021 17:45	EM712 Shallow-water Multibeam Echosounder	information	54° 22,490' N	008° 02,661' E	19,3
MSM98/2_32-1	19.02.2021 17:49	Sound Velocity Profiler	max depth/on ground	54° 22,490' N	008° 02,664' E	19,6
MSM98/2_31-2	19.02.2021 17:52	EM712 Shallow-water Multibeam Echosounder	information	54° 22,490' N	008° 02,662' E	19,2
MSM98/2_33-1	19.02.2021 21:33	Sound Velocity Profiler	max depth/on ground	54° 22,314' N	008° 02,632' E	18,5
MSM98/2_34-1	20.02.2021 01:40	Sound Velocity Profiler	max depth/on ground	54° 24,918' N	008° 02,723' E	19,2
MSM98/2_31-1	20.02.2021 01:50	Multibeam	information	54° 24,815' N	008° 02,897' E	19,9
MSM98/2_35-1	20.02.2021 04:56	Sound Velocity Profiler	max depth/on ground	54° 22,340' N	008° 03,006' E	19,7
MSM98/2_31-1	20.02.2021 05:00	Multibeam	information	54° 22,340' N	008° 03,006' E	19,6
MSM98/2_36-1	20.02.2021 09:38	Sound Velocity Profiler	max depth/on ground	54° 22,351' N	008° 03,076' E	17,6
MSM98/2_31-1	20.02.2021 09:43	Multibeam	information	54° 22,351' N	008° 03,076' E	17,4
MSM98/2_31-3	20.02.2021 11:28	Multibeam	profile start	54° 24,875' N	008° 02,554' E	17,9

MSM98/2_31-3	20.02.2021 11:44	Multibeam	profile end	54° 24,706' N	008° 02,716' E	18,5
MSM98/2_37-1	20.02.2021 11:59	Grab	max depth/on ground	54° 24,534' N	008° 02,737' E	19,1
MSM98/2_37-2	20.02.2021 12:03	Grab	max depth/on ground	54° 24,534' N	008° 02,736' E	19,2
MSM98/2_38-1	20.02.2021 12:33	Grab	max depth/on ground	54° 24,532' N	008° 02,726' E	19,2
MSM98/2_39-1	20.02.2021 13:04	Grab	max depth/on ground	54° 23,140' N	008° 02,847' E	19,3
MSM98/2_40-1	20.02.2021 13:29	Grab	max depth/on ground	54° 22,563' N	008° 02,953' E	18,4
MSM98/2_41-1	20.02.2021 13:35	Sound Velocity Profiler	max depth/on ground	54° 22,563' N	008° 02,954' E	18,7
MSM98/2_42-1	20.02.2021 15:18	Sound Velocity Profiler	max depth/on ground	54° 22,274' N	008° 02,862' E	20
MSM98/2_31-1	20.02.2021 15:21	Multibeam	information	54° 22,274' N	008° 02,862' E	20
MSM98/2_31-4	20.02.2021 15:22	Parasound P70	profile start	54° 22,274' N	008° 02,862' E	20,1
MSM98/2_31-2	20.02.2021 15:22	EM712 Shallow-water Multibeam Echosounder	information	54° 22,274' N	008° 02,862' E	20,1
MSM98/2_31-1	20.02.2021 17:35	Multibeam	profile end	54° 22,584' N	008° 02,618' E	19,4
MSM98/2_43-1	20.02.2021 17:40	Sound Velocity Profiler	max depth/on ground	54° 22,494' N	008° 02,618' E	19,6
MSM98/2_44-1	20.02.2021 22:40	Sound Velocity Profiler	max depth/on ground	54° 25,976' N	007° 26,371' E	28
MSM98/2_45-1	20.02.2021 22:52	Multibeam	information	54° 25,784' N	007° 25,938' E	28,3
MSM98/2_46-1	21.02.2021 01:22	Sound Velocity Profiler	max depth/on ground	54° 25,590' N	007° 27,178' E	28,6
MSM98/2_45-3	21.02.2021 01:40	EM712 Shallow-water Multibeam Echosounder	profile start	54° 25,617' N	007° 26,275' E	28,9
MSM98/2_47-1	21.02.2021 06:05	Sound Velocity Profiler	max depth/on ground	54° 25,712' N	007° 26,482' E	29
MSM98/2_45-3	21.02.2021 06:08	EM712 Shallow-water Multibeam Echosounder	information	54° 25,708' N	007° 26,483' E	29
MSM98/2_45-2	21.02.2021 06:08	Multibeam	information	54° 25,707' N	007° 26,484' E	29,1
MSM98/2_48-1	21.02.2021 09:11	Grab	max depth/on ground	54° 26,719' N	007° 24,282' E	29,4
MSM98/2_49-1	21.02.2021 09:16	Grab	max depth/on ground	54° 26,719' N	007° 24,281' E	29,2
MSM98/2_50-1	21.02.2021 09:50	Grab	max depth/on ground	54° 25,254' N	007° 25,320' E	28,3
MSM98/2_45-2	21.02.2021 09:54	Multibeam	information	54° 25,254' N	007° 25,319' E	28,5
MSM98/2_45-3	21.02.2021 09:55	EM712 Shallow-water Multibeam Echosounder	information	54° 25,255' N	007° 25,319' E	28,4
MSM98/2_45-2	21.02.2021 13:29	Multibeam	profile end	54° 25,874' N	007° 26,633' E	28
MSM98/2_51-1	21.02.2021 13:38	Sound Velocity Profiler	max depth/on ground	54° 25,726' N	007° 26,843' E	28,3
MSM98/2_52-1	21.02.2021 14:04	Parasound P70	profile start	54° 25,729' N	007° 26,119' E	28,7
MSM98/2_52-2	21.02.2021 14:04	EM712 Shallow-water Multibeam Echosounder	profile start	54° 25,729' N	007° 26,119' E	28,7
MSM98/2_52-2	21.02.2021 20:00	EM712 Shallow-water Multibeam Echosounder	profile end	54° 27,631' N	007° 31,078' E	26,8
MSM98/2_52-1	21.02.2021 22:00	Parasound P70	profile end	54° 26,940' N	007° 26,917' E	28,9

8 Data and Sample Storage and Availability

The hydro-acoustic data are archived on a dedicated server at Kiel University. In addition, they have been submitted to the BSH database. The data are available except for the dedicated survey areas Tampen-Aegir and the ones in the German Bight both having a moratorium of three years.

The cores are stored and archived in the Kiel core repository. The MSM98/2 scientific party has a three-year moratorium for exclusive analytical work before the cores will be available for sampling by other scientists upon reasonable statement. All data measured at the cores will be included in the PANGAEA data base in Bremerhaven, which will then provide long-term archival and access.

Tab. 8.1 Overview of data availability

Type	Database	Available	Free Access	Contact
Multichannel seismics	Kiel University	Feb 2021	Feb 2024	sebastian.krastel@ifg.uni-kiel.de
Subbottom profiling	DAM/BSH	Feb 2021	Feb 2024	sebastian.krastel@ifg.uni-kiel.de
Multibeam Bathymetry and SVP	DAM/BSH/ PANGAEA	Feb 2021	Feb 2024	jens.schneider@ifg.uni-kiel.de
Cores and Grabs	Kiel University	Feb 2021	Feb 2024	sebastian.krastel@ifg.uni-kiel.de

9 Acknowledgements

We would like to thank Captain Ralf Schmidt and the entire crew of R/V MARIA S. MERIAN for the excellent support during our cruise, for the hospitality and professional support throughout the cruise. We also acknowledge the support from the German Research Fleet Coordination Centre with organization and help during preparation and conduction of the cruise. The expedition was funded by the German Research Foundation (DFG).

10 References

Barrett, R. S., Bellwald, B., Talling, P. J., Micallef, A., Gross, F., Berndt, C., …, Krastel, S., 2020. Does retrogression always account for the large volume of submarine megaslides? Evidence to the contrary from the Tampen Slide, offshore Norway. Journal of Geophysical Research: Solid Earth, e2020JB020655.

Barrett, R., Bellwald, B., Talling, P., Gross, F., Berndt, C., Micallef, A., Planke, S., Myklebust, R., Krastel, S., 2020. Does retrogression always account for the large volume of submarine megaslides? Evidence to the contrary from the Tampen Slide, Offshore Norway. JGR: Solid Earth 126(2).

Hjelstuen, B.O., Andreasson, E.V., 2015. North Atlantic Ocean deep-water processes and depositional environments: A study of the Cenozoic Norway Basin. Marine and Petroleum Geology 59: pp. 429-441.

King, E.L., Sejrup, H.P., Haflidason, H., Elverhøi, A., Aarseth, I., 1996. Quaternary seismic stratigraphy of the North Sea Fan: glacially-fed gravity flow aprons, hemipelagic sediments, and large submarine slides. Marine Geology, 130(3–4): pp. 293–315.

Karstens, J., Schneider von Deimling, J., Böttner, C., Elger, J., Hilbert, H. S., Kühn, M., ... & Schramm, B. (2018). RV ALKOR Cruise Report 512 [AL512]-North Sea Blowouts, 15th July-26th July, 2018, Cuxhaven-Kiel (Germany).

Krämer, K., Holler, P., Herbst, G., Bratek, A., Ahmerkamp, S., Neumann, A., …, Winter, C., 2017. Abrupt emergence of a large pockmark field in the German Bight, southeastern North Sea. Scientific reports, 7(1), pp. 1-8.

Laberg, J.S., Vorren, T.O., 2000. The Trænadjupet Slide, offshore Norw–y - Morphology, evacuation and triggering mechanisms. Marine Geology, 171(1–4): pp. 95–114.
Lekens, W.A.H., Haflidason, H., Seirup, H.P., Nygard, A., Richter, T., Vogt, C., Frederichs, T., 2009. Sedimentation history oft he northern North Sea Margin during the last 150 ka. Quarernary Science Review, 28(5-6): pp. 469-483.
Lohrberg, A., Krastel, S., Unverricht, D., Schwarzer, K., 2021. The Heligoland Glacitectonic Complex in the southeastern North Sea: indicators of a pre-or early-Elsterian ice margin. Boreas.
Lohrberg, A., Schwarzer, K., Unverricht, D., Omlin, A., Krastel, S., 2020. Architecture of tunnel valleys in the southeastern North Sea: new insights from high-resolution seismic imaging. Journal of Quaternary Science, 35(7), pp. 892-906.
Nygård, A., Sejrup, H.P., Haflidason, H., Bryn P., 2005. The glacial North Sea Fan, southern Norwegian Margin: Architecture and evolution from the upper continental slope to the deep-sea basin. Marine and Petroleum Geology 22(1-2): pp. 71–84.
Pope, E.L., Talling, P.J., Ó Cofaigh, C., 2018. The relationship between ice sheets and submarine mass movements in the Nordic Seas during the Quaternary. Earth Science Reviews178: pp. 208–256.
Watts, C.J., 2019. Submarine mega-slides from the Norwegian Continental margin and their relationship to periods of climatic change. University of Southampton, Doctoral Thesis, 235pp.
Winsemann, J., Koopmann, H., Tanner, D. C., Lutz, R., Lang, J., Brandes, C., Gaedicke, C., 2020. Seismic interpretation and structural restoration of the Heligoland glaciotectonic thrust-fault complex: Implications for multiple deformation during (pre-) Elsterian to Warthian ice advances into the southern North Sea Basin. Quaternary Science Reviews, 227, 106068.

11 Appendices

11.1 Selected Pictures of Samples

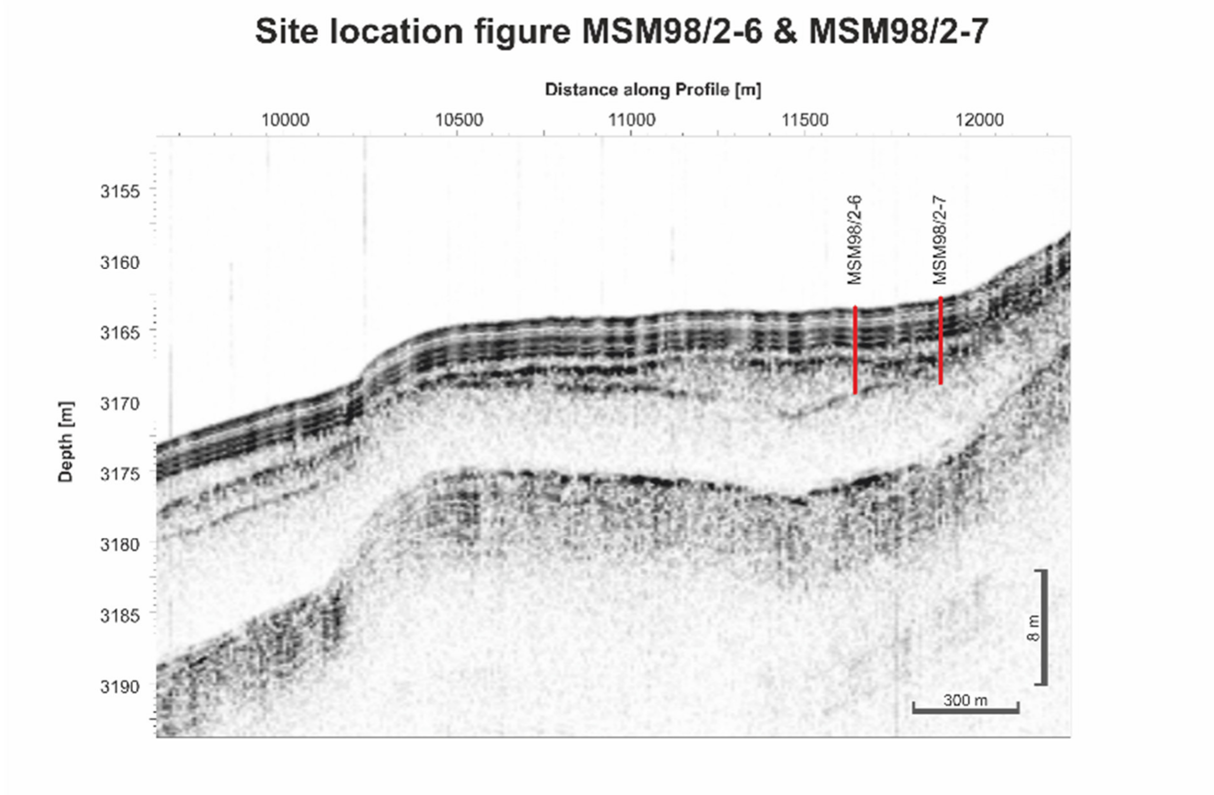

MSM98/2-6

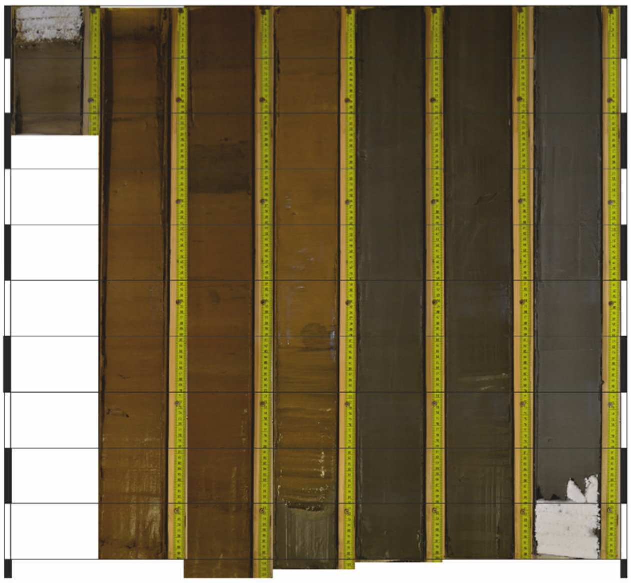

MSM98/2-7

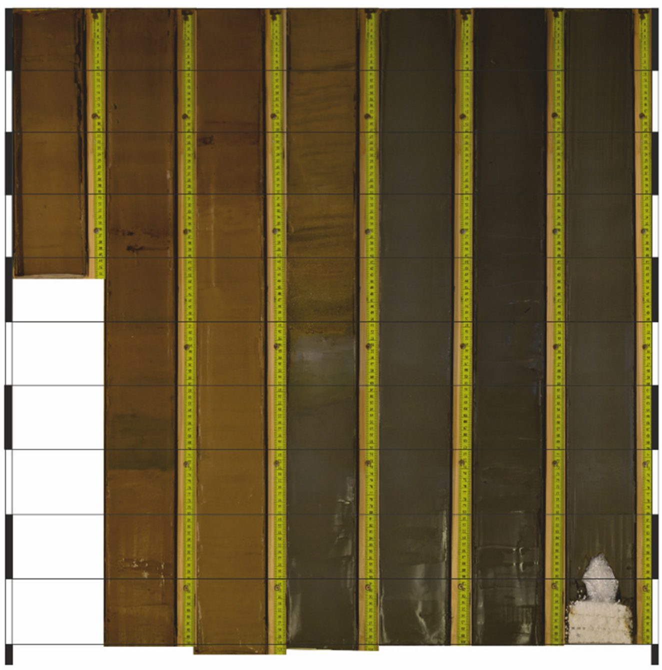

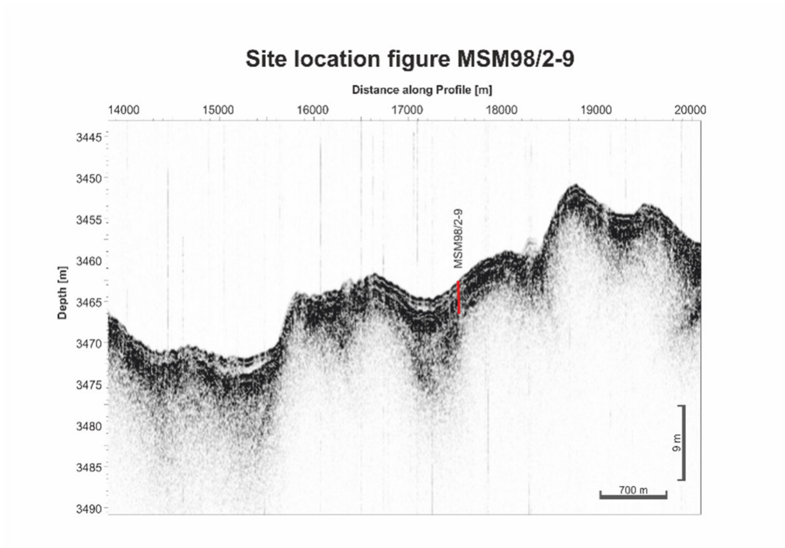
Site location figure MSM98/2-9
Distance along Profile [m]
14000
15000
16000
17000
18000
19000
20000
Depth [m]
3445
3450
3455
3460
3465
3470
3475
3480
3485
3490
MSM98/2-9
9 m
700 m


MSM98/2-9

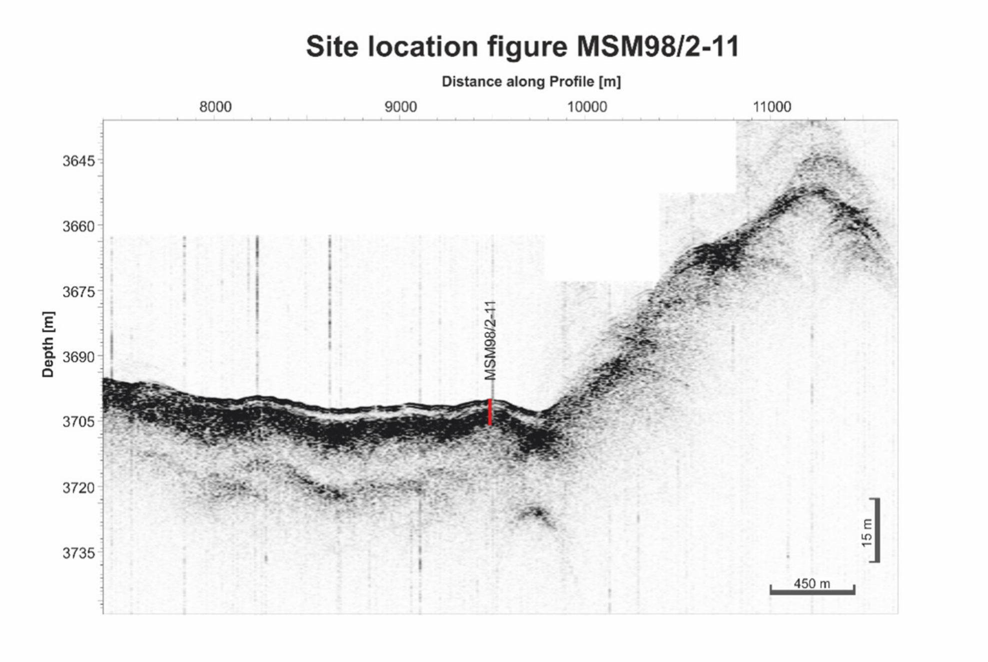
Site location figure MSM98/2-11
Distance along Profile [m]
8000
9000
10000
11000
Depth [m]
3645
3660
3675
3690
3705
3720
3735
MSM98/2-11
15 m
450 m

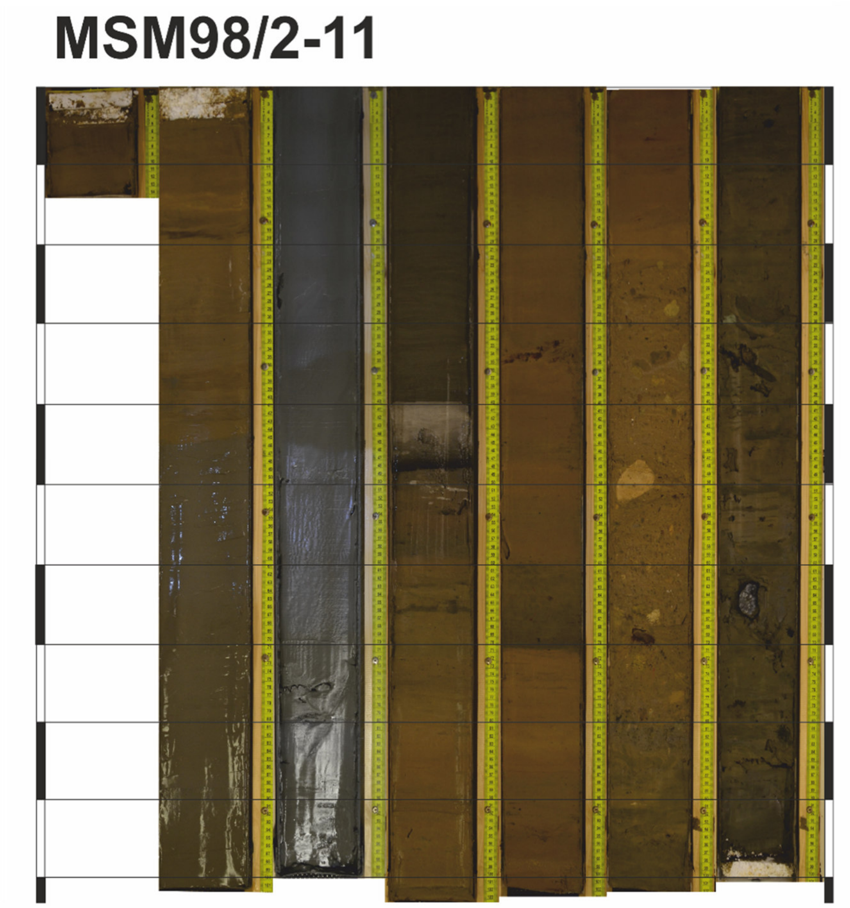
MSM98/2-11

Site location figure MSM98/2-17 & MSM98/2-18 & MSM98/2-19

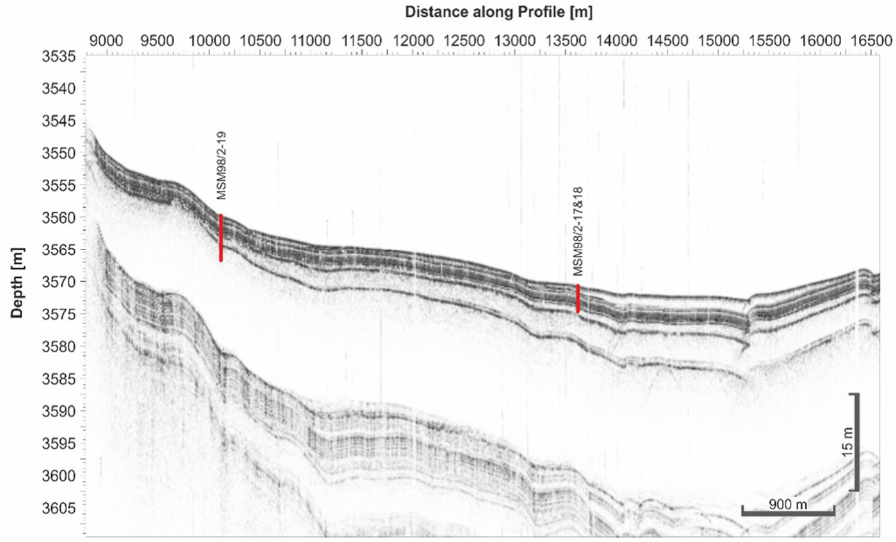

MSM98/2-17

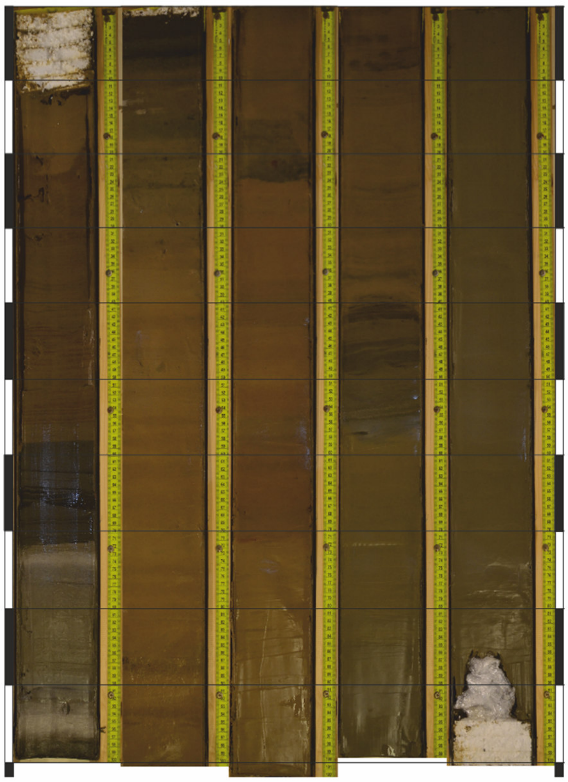

MSM98/2-18

MSM98/2-19

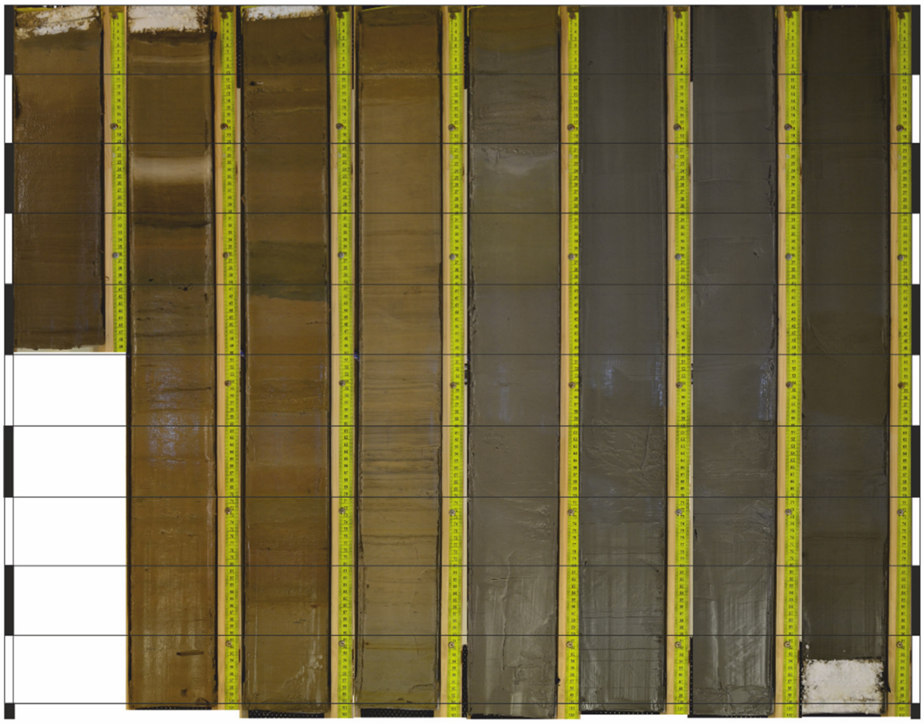

MSM98/2-37-1

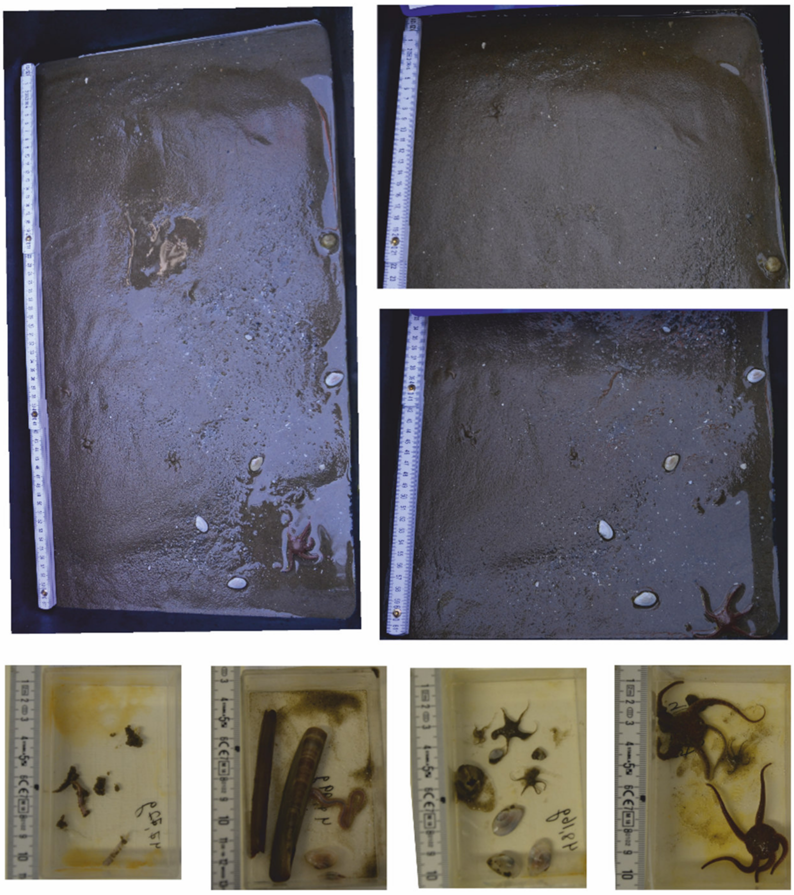

MSM98/2-37-2

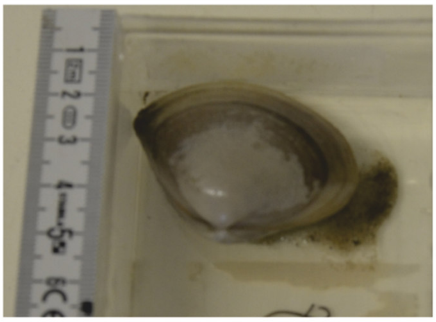

MSM98/2-38-1

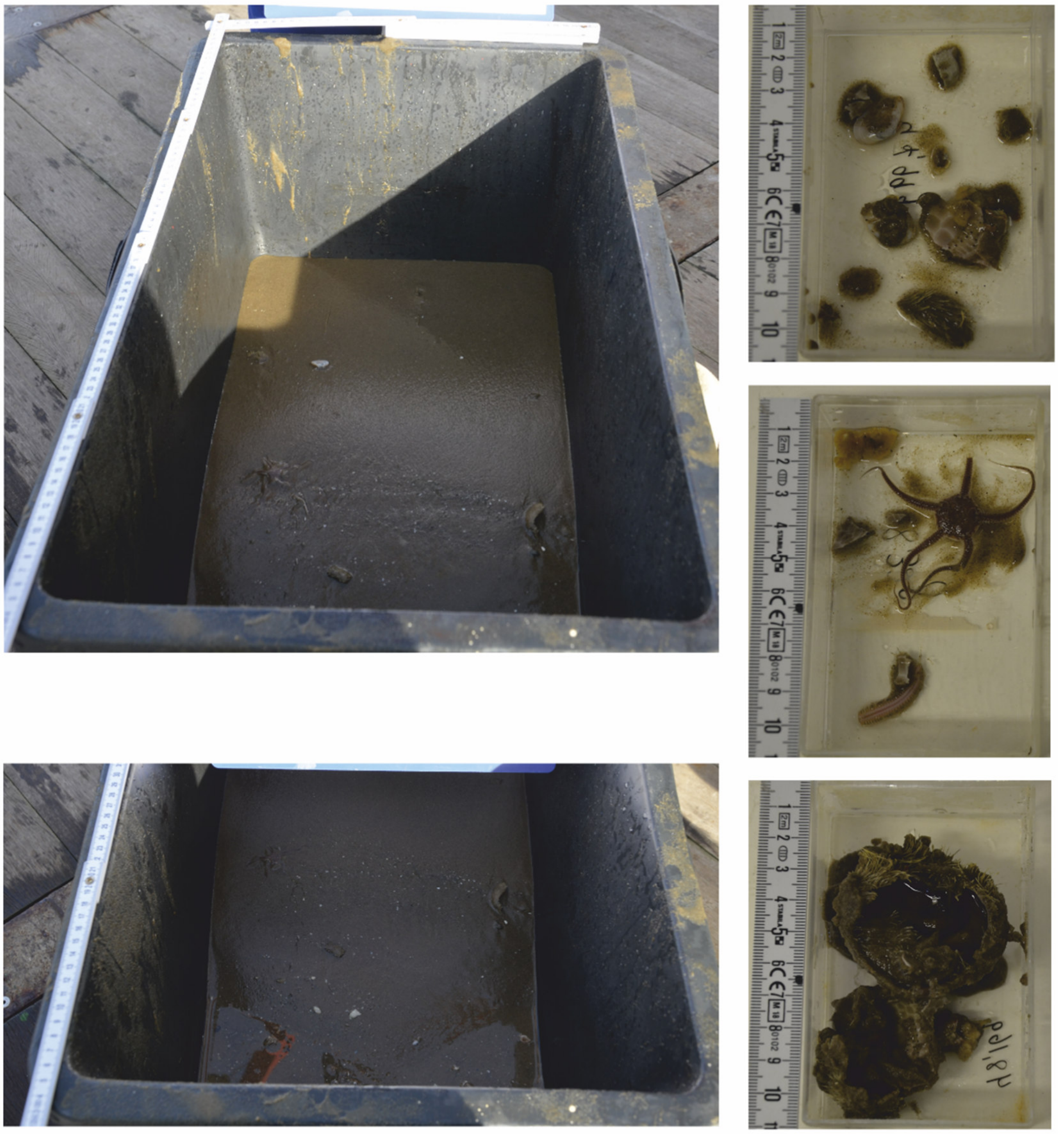

MSM98/2-39-1

MSM98/2-40-1

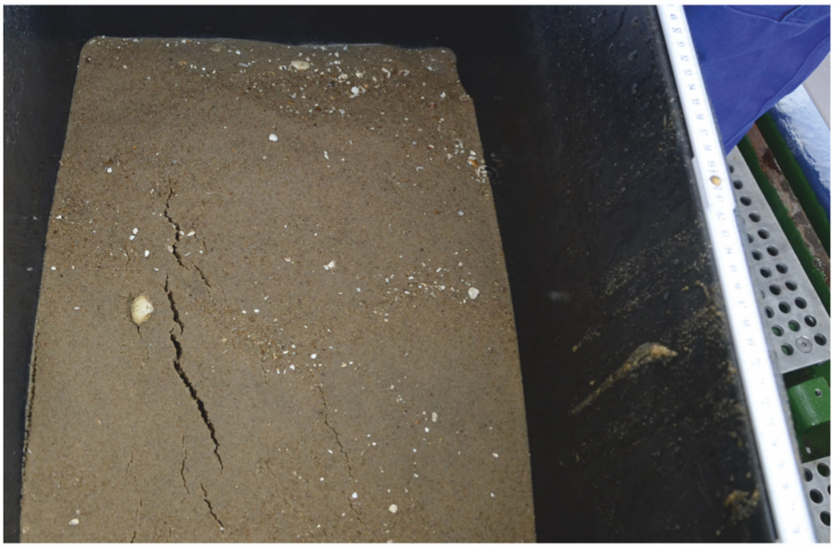

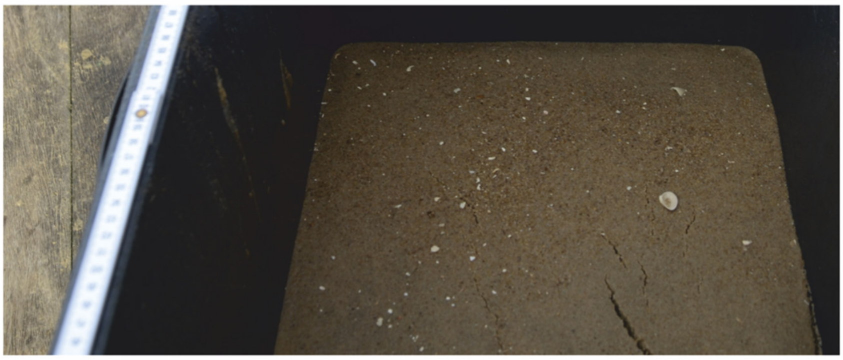

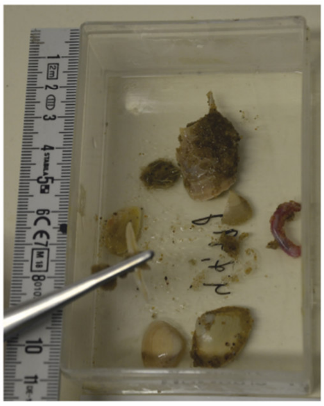

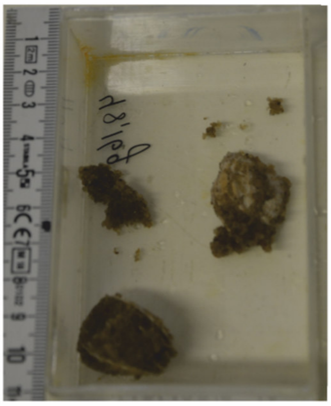

MSM98/2-48-1

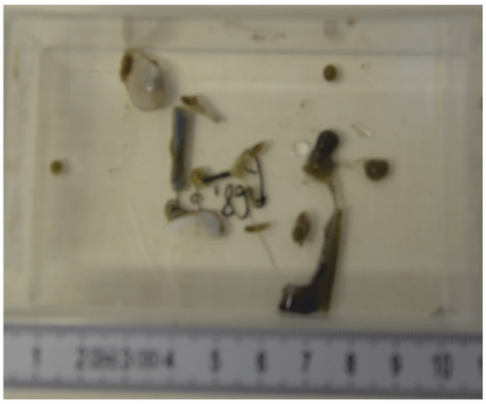

MSM98/2-49-1

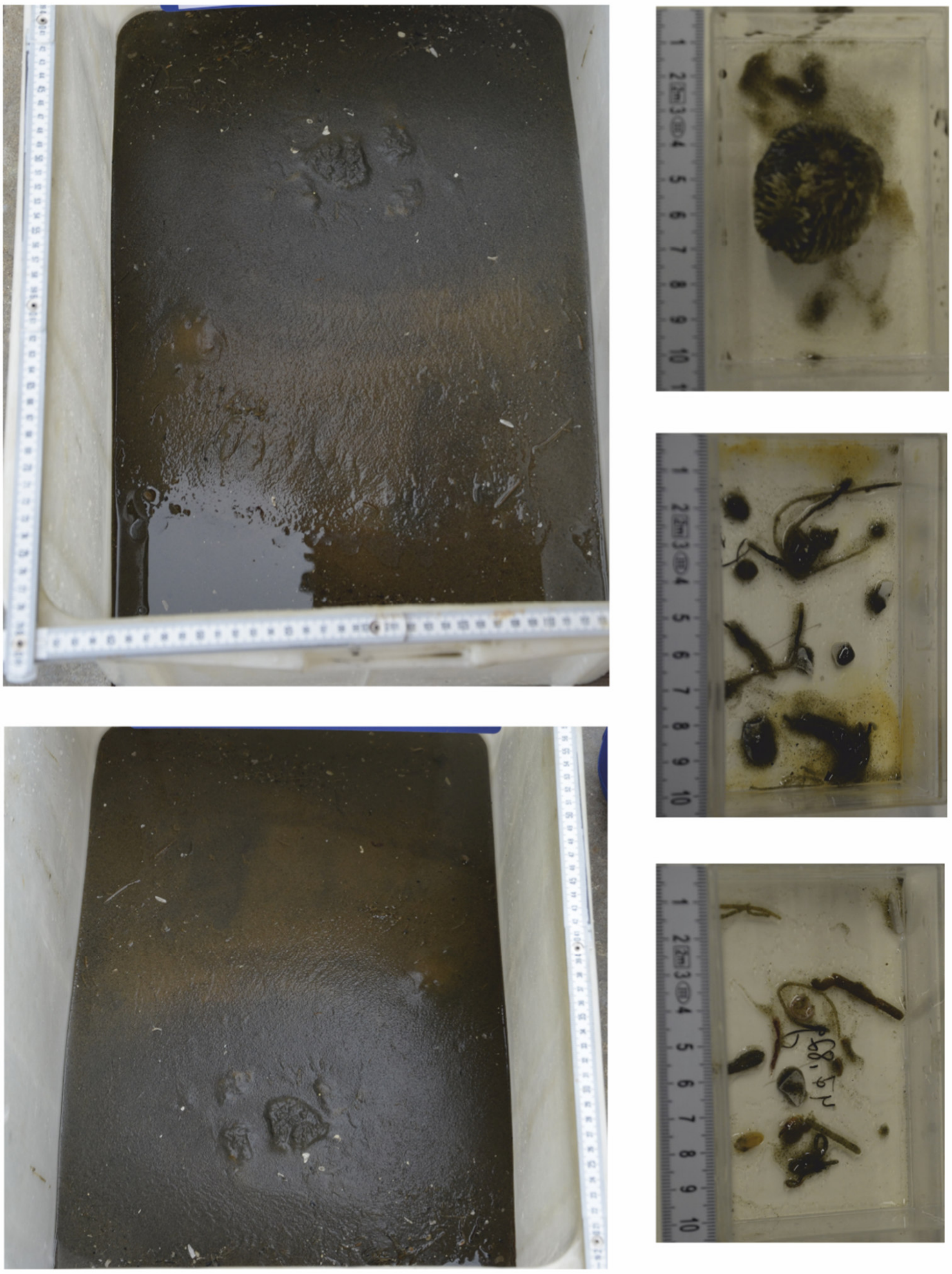

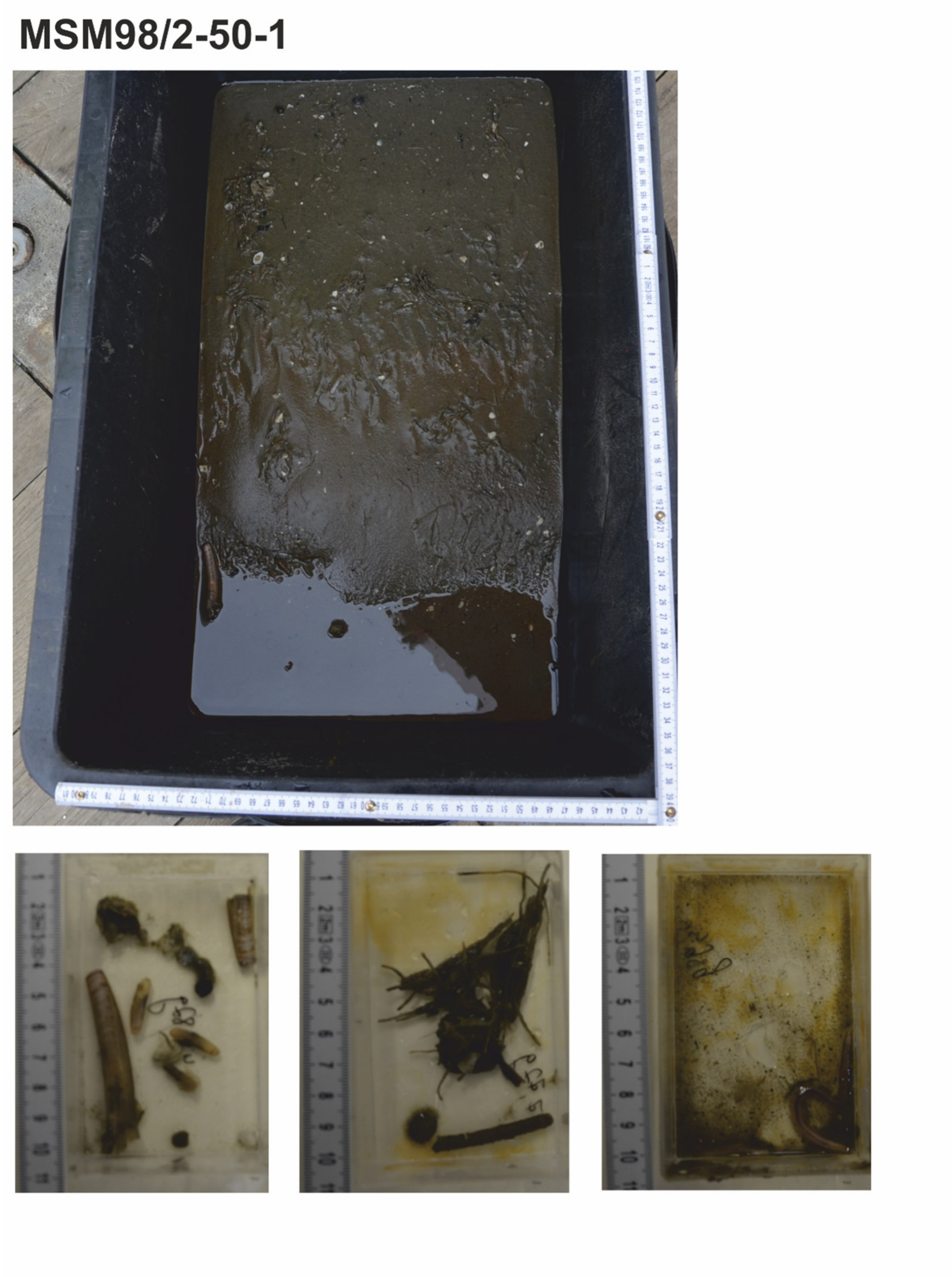

11.2 Scripts

```
#!/bin/bash
# 2021 Jens Schneider
# convert BSH oceanographic elevation_current model data to MBSystem tide format also loadable in Qimera
# use BSH_model_file as first argument, e.g. call
#
```

```
#  Input:  BSH model data, e.g. bsh_elev_currents.dat
#
#  SYNTAX  ./bsh2mbsystem_tide.bash bsh_elev_currents_testfile.dat
#
#  Output: writes and overrites "tide_mbsystem.txt"

FILE_IN=$1
FILE_OUT=tide_mbsystem.txt

echo ""
echo "*******************************************************"
echo "converting ${FILE_IN}"
# store coordinates for header
head1=`head -n1 ${FILE_IN}`

# remove the header of BSH data
awk 'NR>4 {print t} {t=$0}' ${FILE_IN} > ${FILE_OUT}.$$

# split into columns and reformat
awk '{print $1}' ${FILE_OUT}.$$ > ${FILE_OUT}.1
sed 's/\./ /g' ${FILE_OUT}.1 > ${FILE_OUT}.1f
awk '{print $2}' ${FILE_OUT}.$$ > ${FILE_OUT}.2
sed 's/\:/ /g' ${FILE_OUT}.2 > ${FILE_OUT}.2f
awk '{print $6}' ${FILE_OUT}.$$ > ${FILE_OUT}.3f
#use space instead of TAB and separate by three consequtive spaces to meet MBSystem format
specifications
paste -d"\ " ${FILE_OUT}.1f ${FILE_OUT}.2f ${FILE_OUT}.3f > ${FILE_OUT}.4

awk '{print $3, $2, $1, $4, $5, "00","   "$6}' ${FILE_OUT}.4 > ${FILE_OUT}.5
# prepend variable content to line 1 as header
cat <(echo "# $head1") ${FILE_OUT}.5 > ${FILE_OUT}
echo "MB-System tide file $FILE_OUT has been written"
echo "$FILE_OUT can  be loaded in Qimera by custom tide file import"
echo -e "*******************************************************\n"

rm ${FILE_OUT}.*
```